Merging experimental design and structural identification around the concept of modified Constitutive Relation Error in low-frequency dynamics for enhanced structural monitoring

Matthieu Diaz, Pierre-Étienne Charbonnel, Ludovic Chamoin

Merging experimental design and structural identification around the concept of modified Constitutive Relation Error in low-frequency dynamics for enhanced structural monitoring

M. Diaz[a,*], P.-É. Charbonnel[b], L. Chamoin[a,c]

[a] *Université Paris-Saclay, CentraleSupélec, ENS Paris-Saclay, LMPS - Laboratoire de Mécanique Paris-Saclay, 91190, Gif-sur-Yvette, France*

[b] *DES-Service d'Études Mécaniques et Thermiques (SEMT), CEA, Université Paris-Saclay, 91191 Gif-sur-Yvette, France*

[c] *IUF, Institut Universitaire de France*

Abstract

The modified Constitutive Relation Error (mCRE) is a model updating functional in which structural parameters are sought alongside mechanical fields as the best trade-off between all available information given by measured data and physics knowledge, without any further assumptions. Its robustness to measurement noise and remarkable convexity properties make it a credible alternative to classical model updating methods. However, the model updating process is still conditioned by the number and location of sensing devices, which makes damage detection in SHM applications a challenging task as the available measurements are usually spatially sparse. The question of optimal sensor placement (OSP) has been largely addressed in the last decades with various strategies that aim at optimizing sensors locations either for modal analysis or structural identification. In this paper, we propose an alternative to these techniques with a new sensor placement strategy dedicated to mCRE-based model updating. It uses the concept of Information Entropy by formulating a modified Fisher information matrix, using the strong connection between mCRE and Bayesian inference. A proof of concept involving an earthquake engineering inspired academic case study, where accelerometers are positioned on a two-story frame structure subjected to random ground motion, permits to illustrate the soundness and efficiency of the proposed methodology compared to other classical OSP techniques. The influence of critical mCRE parameters is shown, as well as the benefits of taking multiple scenarios into account so as to get an OSP that is relevant for a wider range of possible damage occurences.

Keywords: Optimal Sensor Placement, Modified Constitutive Relation Error, Structural Health Monitoring, Damage Detection, Earthquake Engineering.

*Corresponding author

Email address: matthieu.diaz@ens-paris-saclay.fr (M. Diaz)

1. Introduction

Structural Health Monitoring (SHM) aims to improve the diagnosis of structures in operational conditions in order to prevent potential structural failures. If the monitoring operation was traditionally performed visually by human inspectors, the automated techniques that have been developed in the last four decades, which directly exploit data acquired by a set of sensors, make it possible to assist and reinforce the visual inspection carried out on structures in order to permit a safe decision-making process. SHM has been particularly studied in the context of localizing, quantifying, and tracking structural damage from ambient dynamic datasets. Throughout the last decades, a broad panel of damage detection methods has been proposed [1, 2, 3, 4] - only to cite a few of them. These techniques all have in common the aim of updating numerical models, whether they are directly built from measurements (*black-box modeling*) or derived after an in-depth physical description of the involved phenomena (*white-box modeling*). These latter are then post-processed to extract valuable information regarding the current mechanical state of the sensed specimen, for instance, stiffness loss or modal feature changes [5, 6].

When performing model updating from (possibly spatially sparse) datasets, several difficulties have been identified [7, 8, 9]:

(i) Model bias due to the fact that the chosen class of structural models does not contain the actual behavior of the structure;
(ii) Measurement noise in the dynamic test data that implies the addition of *a priori* information for regularization purposes;
(iii) Incomplete observability of the structure due to the limited budget and technologies of available sensing devices, leading to local and incomplete datasets;
(iv) Incomplete number of contributing modes due to limited bandwidth in the input and dynamic response.

As difficulties (i) and (iv) are already addressed throughout the model updating framework considered in this contribution, we will mainly focus on the difficulty (iii) as one shall imagine how inappropriate experimental designs can lead to inaccurate identification results.

The will to exploit at best the information provided by a few amount of sensors lead to the development of optimal sensor placement (OSP) techniques to guarantee the relevance of sensors locations for various applications such as modal identification, structural identification, or damage detection. Indeed, the quality of damage diagnosis from structural vibrations critically depends on the sensor layout, in particular when a small number of sensors is used for large structures under unknown or random excitation. It is especially the case of large-scale civil structures such as bridges or buildings that cannot be fully instrumented in practice. As part of the experimental design, OSP is a challenging problem. Indeed, as sensors are not properly positioned at this stage, actual measurements are not available. The performance of OSP algorithms is thus conditioned by the (assumed good) predictive behavior of the involved numerical models that allow to generate simulated data. Besides, it is also an expensive task from the computational viewpoint due to the numerous calls to data generation simulations. The question of sensor placement is not new [10, 11] and has been massively studied in the last three decades for SHM applications [12, 13, 14, 15] with the introduction of a wide variety of OSP criteria and optimization algorithms.

In SHM and structural dynamics applications, OSP problems were initially raised for modal identification purposes, as it has been historically well-known that damage occurrence was strongly related to eigenfrequencies loss and mode shapes change [16]. Reference [17] is one of the first papers devoted to OSP for parameter estimation of structures subjected to earthquake loading conditions. Authors exhibit a mathematical expression of the OSP problem for a given amount of sensors that has been reinvested in many other works [18, 19, 20]. In particular,

the Fisher Information Matrix (FIM) has been exhibited from the Cramér-Rao bound theorem and optimized for OSP as it is directly related to the covariance of the model parameters to update. The FIM is a relevant mathematical entity on which the sensor selection process can rely as it is a way of measuring the amount of information carried by a given sensor configuration (since it is strongly related to the sensitivity of model predictions with respect to the updated parameters). FIM-based OSP algorithms differ in the criterion/measure derived from the FIM. The most common approaches are based on:

- ▷ the trace of the FIM - also referred to as A-optimality. The trace is a measure of the global sensitivity of the sensors with respect to the parameters and hence has to be maximized. It has been the optimality criterion used in the pioneering works of Udwadia and co-workers [17, 21] and reinvested by Heredia-Zavoni to perform OSP for buildings submitted to ground motion [20, 22].
- ▷ the condition number of the FIM - also referred to as E-optimality. The condition number is related to the rank of the FIM matrix and to the difficulty in performing its inversion. The minimization of the condition number of the FIM ensures that no sensor is redundant with another [23] as it preserves the rank of FIM.
- ▷ the determinant of the FIM - also referred to as D-optimality. The inverse of the determinant is a measure of the overall uncertainty on the estimated parameters, which thus needs to be minimized. For instance, one can mention the Effective Independence method (EI) developed by Kammer and co-workers [19, 24] where attention is paid to the sensitivity of the mode shape matrix.

Contrary to the previous OSP techniques that are based on modal features, the Bayesian framework proposed by Beck and Katafygiotis [25, 26] has been used to get OSP for structural identification by Papadimitriou [27] using the concept of Information Entropy (IE). It benefits from the Bayesian statistical framework as it properly handles measurement uncertainties as well as model errors. A significant mathematical result relates asymptotically (*i.e.* for a large amount of data) the IE to the determinant of the FIM [28].

From these pioneering works, the research in OSP in the last decade has mostly been focused on optimization algorithms, as optimal sensor placement is a challenging problem from the computational viewpoint which resorts to combinatorial optimization. Efficient algorithms (that may provide sub-optimal results) are often used. They can be distinguished into two families. On the one hand, metaheuristic algorithms such as Genetic Algorithms (GAs) are most suitable for solving discrete optimization problems and providing near-optimal solutions to global optimization problems [24, 27]. Ref. [29] presents an OSP strategy dedicated to damage detection from mode shape variations using an improved GA in which the mutation of populations is constrained. Ref. [30] gathered four sensor placement criteria altogether using a genetic algorithm within a dedicated numerical interface to facilitate OSP. Recently, [31] proposes a FIM-based sensor placement strategy using GA for optimal (in the statistical sense) damage detection from output-only measurements. Neural Networks (NN) are also valuable tools for sensor placement [32]. Ref. [33] describes an approach for fault detection and classification using neural networks and GAs, showing good agreement between both approaches. Of course, the use of metaheuristic/exploratory optimization algorithms does not restrict to GA and NN. For example, one can refer to sensor placement techniques inspired by topological optimization [34, 35], simulated annealing [33, 36] or mixed variable programming [37]. A comprehensive review of these techniques is given in [15]. On the other hand, sequential sensor placement techniques, whether they are forward (FSSP) or backward (BSSP), do only provide suboptimal sensor configurations. However, they are much less computationally demanding compared to GAs. In practice, the positions of the sensors are determined iteratively by placing/removing one sensor at a time. Though the EI method [19] lies on a BSSP strategy, FSSP and BSSP

have strongly been popularized for IE-based OSP [28, 38, 39]. It has been shown that FSSP and BSSP provide a good approximation (yet suboptimal) of the OSP on many test cases with less computational effort than GAs.

As the wide spectrum of existing OSP strategies is oriented towards modal analysis or structural identification, the ambition of this work is to propose an alternative to these techniques with a strategy dedicated to the use of the modified Constitutive Relation Error functional (mCRE) for finite element model updating.

Indeed, the solution of inverse problems is classically performed using either Bayesian approaches (for which a comprehensive review is available in [5]) or deterministic methods [7, 40]. In these latter approaches, the need for regularization techniques is mandatory to circumvent the ill-posedness of the problem [8]. Although easy to implement, they may lack of robustness in the choice of the *a priori* information that regularizes the solution of the inverse problem in Tikhonov's sense. Moreover, achieving a correct balance of the different terms contributing to the cost function can be a difficult task [41]. However, this user's *a priori* expertise is of paramount importance as it conditions the obtained solution and the convergence of the optimization algorithms [42, 43]. An alternative then consists in using the concept of modified Constitutive Relation Error (mCRE) whose physics-based construction avoids the need for user-dependent knowledge [44, 45, 46]. This is the main driver behind its selection as a reference method for model updating in this paper.

Initially proposed for model updating in dynamics by Ladevèze and co-workers [47, 48], the mCRE functional is defined as a quadratic data-to-model distance enriched with a term based on the concept of Constitutive Relation Error (CRE) [49]. This CRE term is built from the reliability of information concept, and therefore carries a strong mechanical content. In particular, it allows to avoid the direct use of regularization terms based on some *a priori* expert-user knowledge. This functional is known for having enhanced convexity properties [50] and high-robustness to measurement noise [51, 46]. Besides, the elementary contributions of the CRE term can be easily computed. It enables to restrain the updating process to a few parameters and to get direct information on the modeling error [52]. This can be computationally helpful and regularizing (in Tikhonov's sense) when the number of parameters to update becomes important. The relevance and robustness of the mCRE for model updating have been emphasized in many applications. Among other works, let us mention local defect detection [53, 45, 54], full-field material identification from dense measurements [55, 56] and the recent work of the authors dedicated to low signal-to-noise ratio random measurements [46]. As one can explicitly establish a link between mCRE, deterministic and stochastic functionals, it is also worth mentioning the comparative study between mCRE, Tikhonov-based, and Bayesian damage detection using optical fiber strain measurements performed in [57].

The main contribution of this work consists in the development of a novel sensor placement strategy that integrates the mCRE (interpreted in the Bayesian inference framework) within the information theory. A modified FIM is formulated and its determinant is maximized to position sensors optimally for enhanced mCRE-based model updating purposes. A proof of concept showing the relevance of this new mCRE-based OSP strategy is proposed on a 3D academic example representative of a 2-story frame structure. If this study focuses on the optimal locations of accelerometers following the previous work of the authors [46] and their popularity for earthquake engineering applications, all types of sensors can be easily integrated into the presented framework. This case study allowed to compare the new mCRE-based OSP approach with other classical techniques: the relevance of OSPs is assessed in terms of parameter estimation accuracy using measurements from different scenarios and relative uncertainty, using confidence intervals [52]. The effect of the confidence into measurements coefficient is particularly considered as the calibration of the latter is crucial within the mCRE framework [46]. Physically-meaningful comments from the visual spreading of the sensors on the structure are made to

explain the effect of this parameter on the sensor placement results. The case of multiple damage scenarios is also considered, showing that the additional computational burden carried by such an approach yet enables obtaining more relevant OSP leading to better FE matrices corrections, even when the parameters to identify are highly uncertain.

The remainder of this paper is organized as follows: Section 2 presents an overview of OSP techniques dealing with the concept of FIM, with particular emphasis on the IE concept. Section 3 recalls the basics of the mCRE for FE model updating in dynamics with emphasis on stiffness parameters. Section 4 presents the novel sensor placement approach starting from the mCRE seen from a Bayesian viewpoint. The proof of concept of the mCRE-based OSP algorithms on a 3D frame structure is given in Section 5. Conclusions and prospects are finally drawn in Section 6, suggesting a future use of this sensor placement technique for an on-the-fly model updating framework unified around the concept of mCRE.

2. Optimal sensor placement techniques for SHM at a glance

In this section, the most common and popular sensor placement techniques are briefly presented. Although OSP problems were originally raised for modal identification purposes, the tools that are invested are (for the largest part) all related to the information theory, which will be presented in the following. For the sake of conciseness and clarity, only the material essential to the forthcoming developments is detailed. However, the interested reader is invited to find complementary explanations in the following review papers [12, 13, 14, 15].

2.1. Bayesian framework and Fisher Information Matrix

Without loss of generality, solving an inverse problem aims at updating the internal parameters $\theta \in \Theta$ of a given model $\mathcal{M}$ from the knowledge of a given measurement set $y \in \mathcal{Y}$ made of N_s data acquisition channels of length N obtained under a given loading denoted e. In most SHM applications, measurements are discrete kinematic quantities (displacements, strains, accelerations) that directly derive from the mechanical state predicted by the model $u = \mathcal{M}(\theta, e) \in \mathcal{X}$. The projection operator $\Pi : \mathcal{X} \mapsto \mathcal{Y}$ thus allows to compare explicitly predictions with the available N_s measurements. Classically, measurements are correlated to predictions using the observation equation [18, 21]:

$$y = \Pi(u(\theta)) + w \tag{1}$$

where w is an additive noise assumed to be Gaussian of covariance matrix Σ_w allowing to take into account measurement noise and model discrepancies. In what follows attention is paid to the best choice of sensors locations in order to obtain the best (statistical) identification of θ. Briefly, let us start from the Bayes theorem:

$$\pi(\theta|y) \propto \pi(y|\theta).\pi_0(\theta) \tag{2}$$

$\pi_0(\theta)$ is the prior probability density function (pdf) on parameters constructed from *a priori* knowledge. $\pi(\theta|y)$ is the posterior pdf; this conditional probability is the final result improved by the knowledge of measured data, reducing uncertainty and giving the most likely values of θ. Finally, $\pi(y|\theta)$ is the so-called likelihood pdf, which can be interpreted as a measure of how good the parametrized model succeeds in explaining the observations. With the previous assumptions, the posterior pdf takes the form:

$$\pi(\theta|y, \Sigma_w) \propto \exp\left[-\frac{1}{2}\mathcal{J}\left(\theta, y, \Sigma_w\right)\right].\pi_0(\theta) \text{ with } \mathcal{J}\left(\theta, y, \Sigma_w\right) = \sum_{k=1}^{N} \|\Pi u_k(\theta) - y_k\|^2_{\Sigma_w^{-1}} \tag{3}$$

where $\|\square\|^2_{\Sigma_w^{-1}} = \square^T \Sigma_w^{-1} \square$ refers to the squared Euclidean norm of $\square$ weighted by matrix Σ_w^{-1}. $\mathcal{J}$ is a data-to-model distance allowing to measure the correlation between measurements and

predictions. This functional is also minimized in a deterministic viewpoint to identify optimal parameters (with a complementary regularization to circumvent the ill-posedness of the inverse problem). The sensor placement problem then consists in finding the best projector $\widehat{\Pi}$ which minimizes the covariance on the parameter estimate. Note that, because models are numerically discretized (*e.g.* in the finite element sense), then there is no reason to look for optimal sensors locations in a continuous space. Each sensor position will thus be optimized among a "grid" of all N_d possible sensor locations. Doing so, the OSP problem becomes a combinatorial optimization problem, that is well-known for being exploratory and computationally expensive (if one intends to naively look for a global minimum).

If the Fisher Information Matrix (FIM), denoted Q, was originally introduced as the inverse of the Cramér-Rao bound (of the parameters covariance matrix) [21], it can also be derived from the statistical viewpoint as the variance of the score, *i.e.* the gradient of the log-likelihood function $\pi(y|\theta)$:

$$Q = \mathbf{E}_\theta \left(\left(\frac{\partial \log \pi(y|\theta)}{\partial \theta} \right) \left(\frac{\partial \log \pi(y|\theta)}{\partial \theta} \right)^T \right) \tag{4}$$

with $\mathbf{E}_\theta(\bullet)$ referring to the mathematical expectation operator on θ. Unsurprisingly, the FIM is strongly related to the sensitivity of predictions with respect to the parameters. It is a relevant mathematical entity on which the sensor selection can rely as it is a way of measuring the amount of information carried by a given sensor configuration. This explains why pioneering OSP studies were aiming at maximizing the FIM, in the sense of a certain measure [17, 18, 19, 20]. As mentioned above, A- and D- optimality criteria respectively based on the trace and determinant of Q are the most popular approaches. OSP techniques then differ according to the quantity of interest that is considered.

The Effective Independence method (EI) was introduced by Kammer [19]. It can be considered as a modal-based OSP technique as it exploits the Fisher Information Matrix with the modeshape matrix as quantity of interest, the variations of the latter assumed to be directly related to damage. The starting point of this approach is the Mode Shape Difference method (MSD) which considers sensors as relevant if they are sensitive to mode changes [58, 59]. Parameters θ in this case then correspond to the modal coordinates of eigenmodes. The EI method extends this concept with the independence distribution vector; the contribution of each sensor to the eigenmodes is assessed with the matrix

$$EI = \Phi_s \left[\Phi_s^T \Phi_s \right]^{-1} \Phi_s^T \tag{5}$$

where Φ_s is the modal basis partitioned to the sensors locations. EI can be identified as an orthogonal projector whose rank is equal to the number of target modes. EI can thus be of full rank if the mode partitions resulting from a given sensor placement are linearly independent, which is the objective of EI. The so-called independence distribution vector corresponds to the diagonal terms of EI. It enables to quantify how sensors contribute to modal identification. The EI method has been widely exploited in the literature: the strategy has been quickly extended to take modeling errors into account [60] as well as measurement noise effects [61]. An application to a genetic algorithm (GA) based approach has also been proposed in [24] and the method has been able to position at best 3D accelerometers for modal vibration tests [62]. More recently, it has been coupled with topology optimization-inspired tools [35].

It is also worth mentioning the Modal Kinetic Energy (MKE) method in parallel of MSD and EI as it intends to locate sensors at points of maximum modal kinetic energy [63]. The major advantage of MKE compared to EI is that favorable sensor placements are promoted in areas where the signal-to-noise ratio should be important, which limits the spurious effects of measurement noise when performing modal analysis. Ref. [64] studied the mathematical connections between MKE and EI and compared them for SHM applications, showing IE reveals to be an iterated version of MKE.

2.2. Information Entropy

Contrary to MSD, EI and MKE that are based on the sensitivity of modal features, one can formulate the OSP problem from the Bayesian viewpoint. Indeed, the posterior pdf (3) represents the uncertainty of parameters θ based on the information contained in measurements y. The concept of Information Entropy has been introduced to provide a scalar measure of this uncertainty [27, 28]. It benefits from the Bayesian statistical framework as it properly handles measurement uncertainties as well as model errors. The IE, denoted $h(y)$, is given by

$$h(\Pi, y) = \mathbf{E}_\theta \left(-\log \pi(\theta|y) \right) \tag{6}$$

The IE depends on the available data, and the sensor configuration characterized by Π. OSP is then achieved by minimizing the changes in the IE, which is a unique measure of the uncertainty in the model parameters. A rigorous mathematical description of the IE concept for OSP is given in [27, 28] for the case of small and large uncertainties on the parameters to estimate. A major result that has been shown is the asymptotic result for large amount of available data that relates the IE to the determinant of the FIM. For small uncertainties on θ, choosing a relevant value θ_0 which minimizes the misfit function $\mathcal{J}$ leads to the following approximation when $NN_s \to \infty$:

$$\begin{aligned} h(\Pi, y) \approx H(\Pi, y; \theta_0) &= \frac{1}{2} N_\theta \log 2\pi - \frac{1}{2} \log \det(Q(\Pi, \theta_0, y)) \\ \text{with } Q(\Pi, \theta_0, y) = NN_s \nabla_\theta \nabla_\theta^T (\mathcal{J}(\theta, y, \Sigma_w)) &\approx \sum_{i=1}^{N} \left(\Pi \nabla_\theta u_i\right)^T \left(\Pi \Sigma_w \Pi^T\right)^{-1} \left(\Pi \nabla_\theta u_i\right) \end{aligned} \tag{7}$$

where $N_\theta = \dim(\Theta)$ is the number of parameters, N the number of measured samples and N_s the number of sensors. Using (7), one can thus look for N_s optimal sensors locations $\widehat{\Pi}$ solving:

$$\widehat{\Pi} = \arg\max_{\Pi} \left[\log \det(Q(\Pi, \theta_0, y)) \right] \tag{8}$$

For large model uncertainties, a parameter estimate θ_0 cannot be postulated anymore; consireding for example the case of complex damageable structures, one may not straightforwardly guess where damage will appear first. This implies that the OSP will be sought as:

$$\widehat{\Pi} = \arg\max_{\Pi} \left[\int_\Theta \log \det(Q(\Pi, \theta, y)) \pi_0(\theta) \mathrm{d}\theta \right] \tag{9}$$

It is important to notice that according to the values of the sought parameters, for complex problems and geometries (*e.g.* where the sensitivity of the parameters into the identification process is highly heterogeneous), OSP results may strongly differ from one parameter value to the other. In such cases, one should explore the parameter space (for example with Monte-Carlo sampling) and average the contributions of the FIM computed according to each sample. Of course, that type of approach is more expensive from the computational viewpoint.

One of the strong assets of the IE is that it allows to compare sensor configurations of various size [65], as one can guess that adding sensors is always beneficial, or at least equivalent in terms of carried information. In [28], mathematical classification rules are given on the upper and lower bounds of the IE as a function of N_s allowing to perform sequential placements (see Alg. 1) that are almost as efficient as genetic algorithms, but obtained with much less computational effort.

There have been much use of the IE for OSP in the last two decades. Without being exhaustive, let us mention some significant contributions: in [39], the functional has been extended to take into account the effect of sensors spatial correlation in Σ_w. Similarly, a penalty term to enforce the sparsity of the sensor configuration has been added to the IE [66]. The IE was also used to design optimal characteristics of the excitation e for optimal identification [67]. In [38],

a multi-objective optimization problem was introduced to design an OSP dedicated to a class of models. IE was reinvested for statistical seismic source inversion in [68]. IE was also applied to model identification of periodic structures endowed with bolted joints [69] and to optimal crack identification on plates from strain measurements in [70]. Very recently, the case of multiple damage scenario with modal expansion was considered in [71] to handle virtual sensing under output-only vibration measurements.

Algorithm 1: IE-based Forward Sequential Sensor Placement (FSSP) algorithm

Initialization:
- Grid of all N_d possible sensors locations
- Targeted number of sensors N_s
- $n = 0$ number of selected sensors
- Set of simulated measurements y

while $n < N_s$ **do**
  Consider all possible combinations by adding one new sensor: $\{\Pi_j\}_{j\in[\![1;N_d-n]\!]}$
  for $j \in [\![1; N_d - n]\!]$ **do**
    Evaluate the information entropy IE_j of the sensor configuration given by Π_j
  end
  Identify the sensor configuration $J = \arg\min_{j\in[\![1;N_d-n]\!]} [\log\det(Q(\Pi_j, \theta_0, y))]$
  Store the new sensor of configuration J as the $(n+1)^{th}$ optimal position
end

3. The modified Constitutive Relation Error in dynamics

As explained above, the modified CRE is built as a quadratic data-to-model distance enriched with a term based on the so-called concept of Constitutive Relation Error. The enrichment of the data-to-model distance with a term having strong mechanical content allows to improve the convexity properties of the functional, which provides enhanced robustness to measurement noise. Besides, as the CRE term directly derives from the set of equations that define the dynamics problem under study, it avoids the user-dependent choice of the regularization term that is mandatory to deal with the intrinsic ill-posedness of the identification problem in Hadamard's sense when using traditional approaches.

One of the specificities of the mCRE functional is that both parameters and mechanical fields are identified simultaneously, which leads to a nested minimization problem to solve. The key theoretical ingredients for the formulation and minimization of the mCRE in dynamics when updating stiffness parameters are recalled below. For complementary details and a literature overview of the mCRE, the interested reader is referred to the recent contributions [46, 72].

3.1. FE framework, measurements and stiffness parametrization

Let us consider the general case of an elastic structure Ω spatially discretized in E (non-overlapping) finite elements such that $\Omega = \cup_{e=1}^{E} \Omega_e$ subjected to a given dynamical loading F. We denote by K, D, M the stiffness, damping and mass FE matrices, respectively, while F_ω and U_ω are the frequency counterparts of nodal loading conditions and displacement field. With these notations, the dynamic equilibrium written in the frequency domain at a given angular frequency ω reads:

$$\left[-\omega^2 M + i\omega D + K\right] U_\omega = F_\omega \tag{10}$$

In addition, a set of sensors is used to measure the magnitude of some kinematic quantities (displacement, velocity and/or accelerations). In the frequency domain, assuming measurements are perfect, such information can be written without loss of generality as:

$$\Pi U_\omega = Y_\omega \tag{11}$$

where Y_ω refers to the frequency counterpart of measurements at angular frequency ω, and Π contains zero and integer powers of $i\omega$ to extract displacement field derivatives at corresponding sensors positions.

As the main driver of this report is to perform SHM and damage detection, one can (legitimately) assume that damage can be interpreted as local stiffness loss. Therefore, a convenient manner to parametrize a linear FE problem for damage detection is to parametrize the FE stiffness matrix. The latter is thus decomposed in N_θ non-overlapping subdomains and parametrized as follows:

$$K(\theta) = \sum_{i=1}^{N_\theta} \theta_i K_{0,i} \quad \text{with} \quad K(\theta_0) = \sum_{i=1}^{N_\theta} K_{0,i} \text{ and } \theta \in \Theta \subset \mathbb{R}^{N_\theta} \tag{12}$$

Note that the subdomains can perfectly match with finite elements or gather some of them to reduce the number N_θ of parameters to identify.

3.2. mCRE-based model updating problem in dynamics

Contrary to standard deterministic approaches, the fundamental idea of mCRE-based model updating is to built mechanical fields and to identify structural parameters simultaneously as a trade-off according to all available information (*i.e.*, physics knowledge and measured data). Therefore, there is no need for additional *a priori* information. The starting point of the approach thus consists in classifying, among the data and equations of the mechanical problem, what will be considered as 'reliable' from what should be considered with caution (labelled 'unreliable'). This separation is non-unique and deeply relies on the case study and engineering expertise, although it is also well-known that constitutive relations are (very often) the less reliable equations. The separation of equations for the considered SHM case is given in Tab. 1. Doing so, we define two manifolds: (i) $\mathcal{U}_{ad}$ the so-called kinematically admissible space that contains the FE displacement fields satisfying the boundary conditions and kinematic relations but not necessarily the constitutive equations, and (ii) $\mathcal{D}_{ad}$ the so-called dynamically admissible space containing the FE displacement fields V such that $[-\omega^2 M + i\omega D]U + K(\theta)V = F_\omega$ for all $U \in \mathcal{U}_{ad}$. In other words, $\mathcal{D}_{ad}$ contains the FE displacement fields satisfying both equilibrium and constitutive equations. The reciprocity gap between those two manifolds can be measured using an energy norm - the CRE - that estimates the relevance of a solution couple $s_\omega = (U_\omega, V_\omega) \in \mathcal{U}_{ad} \times \mathcal{D}_{ad}$ with respect to the mechanical problem. With the above notations, the CRE at a given angular frequency ω reads:

$$\zeta_\omega^2(s_\omega, \theta) = \frac{1}{2}(U_\omega - V_\omega)^H K(\theta)(U_\omega - V_\omega) = \frac{1}{2}\left\|U_\omega - V_\omega\right\|_{K(\theta)}^2 \tag{13}$$

	Reliable	**Unreliable**
Model	• Geometry • Boundary conditions • Equilibrium equations • Dissipative constitutive relations	• Elastic constitutive relations
Experiments	• Loading frequencies $\omega/2\pi$ • Sensors locations • Measured inputs F_ω	• Measured outputs Y_ω

Table 1: Distinction between reliable and unreliable information for damage detection from stiffness update in dynamics.

The extension of the CRE concept to unreliable experimental data (see Tab. 1) directly leads to the so-called *modified Constitutive Relation Error* (mCRE). In the latter, the CRE is

extended with a data-to-model distance written in the frequency domain:

$$e_\omega^2(s_\omega, \theta, Y_\omega) \triangleq \zeta_\omega^2(s_\omega, \theta) + \alpha \frac{1}{2} \left\| \Pi U_\omega - Y_\omega \right\|_G^2 \tag{14}$$

α is the confidence into measurement scaling parameter, allowing to give more or less importance to the measurements in the model updating process (particularly regarding the noise level). Its calibration is crucial to obtain relevant mCRE-based model updating results [46]. G is a symmetric positive-definite matrix that guarantees that $\|\square\|_G$ is homogeneous to ζ_ω^2 and equivalent in level. Its choice is much less critical than α. In practice, G is chosen as proportional to the identity matrix and weighted by the first eigenvalue of $K(\theta_0)$.

Finally, the analysis of a single angular frequency may be too restrictive in dynamics, particularly when several eigenmodes are simultaneously excited. The full mCRE functional $\mathcal{J}$ to be minimized is thus obtained by direct integration over a frequency bandwidth D_ω (which stores the essential information about the structure response):

$$\mathcal{J}(\theta, Y) = \int_{D_\omega} z(\omega) e_\omega^2(\widehat{s}(\theta, Y_\omega), \theta, Y_\omega) \, \mathrm{d}\omega \tag{15}$$

where $z(\omega)$ is a frequency weighting normalized function such that $\int_{D_\omega} z(\omega) \, \mathrm{d}\omega = 1$ allowing to modulate the importance of specific frequencies of D_ω and $\hat{s}$ the optimal mechanical fields for a given parameter set and given measurements. In the present formulation of the mCRE in the frequency domain, $\widehat{s}$ at each angular frequency ω is obtained solving:

$$\forall\, \omega \in D_\omega, \quad \widehat{s}_\omega(\theta, Y_\omega) = (\widehat{U}_\omega, \widehat{V}_\omega) = \underset{s \in (\mathcal{U}_{ad} \times \mathcal{D}_{ad})}{\arg\min} \; e_\omega^2(s, \theta, Y) \tag{16}$$

which is a minimization problem constrained by the satisfaction of the dynamic equilibrium between the manifolds $\mathcal{U}_{ad}$ and $\mathcal{D}_{ad}$. In practice, an augmented cost-function with Lagrange multipliers is introduced:

$$\mathcal{L}(U, V, \Lambda, \theta) = \frac{1}{2} \|U - V\|_{K(\theta)}^2 + \frac{\alpha}{2} \|\Pi U - Y\|_G^2 + \Lambda^T \left[[-\omega^2 M + i\omega D] U + K(\theta) V - F \right] \tag{17}$$

which leads to the matrix system written below that must be solved for all ω in D_ω:

$$\Leftrightarrow A \begin{bmatrix} \widehat{\Lambda}_\omega \\ \widehat{U}_\omega \end{bmatrix} = b \text{ with } \begin{cases} \widehat{\Lambda} &= \widehat{U}_\omega - \widehat{V}_\omega \\ A &= \begin{bmatrix} \left[K(\theta) + i\omega D - \omega^2 M \right]^H & \alpha \Pi^H G \Pi \\ -K(\theta) & \left[K(\theta) + i\omega D - \omega^2 M \right] \end{bmatrix} \\ b &= \begin{Bmatrix} \alpha \Pi^H G Y_\omega \\ F_\omega \end{Bmatrix} \end{cases} \tag{18}$$

The overall mCRE-based model updating problem thus reads:

$$\hat{\theta} = \underset{\theta \in \Theta}{\arg\min} \left\{ \mathcal{J}(\theta, Y) \triangleq \int_{D_\omega} z(\omega) e_\omega^2 \left(\left[\underset{s \in \mathcal{U}_{ad} \times \mathcal{D}_{ad}}{\arg\min} \, e_\omega^2(s, \theta, Y_\omega) \right], \theta, Y_\omega \right) \mathrm{d}\omega \right\} \tag{19}$$

3.3. Additional remarks

Although the nested minimization problem (19) on mechanical state and parameters make the algorithmic structure for minimization quite complex compared to classical model updating methods, one should notice that the computation of mechanical fields for a given value of θ is not computationally expensive as the size of (18) can be drastically reduced using projection on reduced truncated modal basis [73].

The minimization of the mCRE with respect to parameters can be numerically performed using unconstrained minimization algorithms such as the BFGS method or the trust-region algorithm. It is worth noticing that there exist analytical expressions of the gradient and Hessian matrix of the mCRE with respect to parameters as well as the gradient of mechanical state with respect to parameters. These expressions are valuable to reduce the computational burden associated to the minimization of the mCRE functional. They are also decisive in the following to improve the numerical performance of the mCRE-based OSP algorithm. All the mathematical developments leading to these expressions in the present parametrization case are given in Appendix A.

If supplying an analytical Hessian matrix may lead to minor computational improvements when minimizing the mCRE, it can still be exploited to compute confidence intervals [52]. Indeed, when identifying several parameters simultaneously, one could wonder what relative precision is reached in the identification process for Uncertainty Quantification (UQ). To do so, one can thus consider the computation of confidence intervals as a first approach. More details are given in Appendix B.

4. A mCRE-oriented OSP strategy

For structures having heterogeneous sensitivity of stiffness to model updating, parameter estimates may be quite far from reality when the model updating process is performed using a small amount of sensors. This is the case for several SHM applications considering one cannot always afford for rich instrumentation on large scale structures. If OSP strategies have been proposed for (standard) structural identification and modal analysis, there is no proper sensor placement strategy dedicated to mCRE-based model updating in the literature whereas it has demonstrated to be an efficient alternative to standard approaches [57]. In the following, we present a modified FIM that integrates the mCRE concept, which is legitimate in light of the link between the mCRE (though deterministic) and the Bayesian inference framework.

4.1. The mCRE from a Bayesian viewpoint

Although the previously introduced mCRE-based model updating strategy is deterministic, one can show that this procedure is equivalent to the Maximum *A Posteriori* (MAP) estimation in the Bayesian inference framework with Gaussian distributions, an error norm based on the measurement error covariance matrix, and no *a priori* on parameters [74, 75]. Since covariance on the modeling error is usually not known, the idea is to integrate modeling error in a different manner into Bayesian inference, in a more global and less strict framework that allows more flexibility in the model structure.

If one assumes that the prior pdf $\pi_0(\theta)$ and the likelihood function $\pi(y|\theta)$ are both defined with Gaussian distributions, then

$$\pi_0(\theta) \propto \exp\left[-\frac{1}{2}\left(\theta-\bar{\theta}\right)^T \Sigma_0^{-1}\left(\theta-\bar{\theta}\right)\right] \tag{20}$$

$$\pi(y|\theta) \propto \exp\left[-\frac{1}{2}\left(\mathcal{M}(\theta,e)-y\right)^T \left[\Sigma_m+\Sigma_y\right]^{-1}\left(\mathcal{M}(\theta,e)-y\right)\right] \tag{21}$$

where $\Sigma_0, \Sigma_m, \Sigma_y$ respectively denote the *a priori*, model and observations covariance matrices. $\bar{\theta}$ is the mean of the prior pdf. Therefore, according to the Bayes theorem (2) and the Maximum A Posteriori principle, the optimal set of parameters can be sought as

$$\hat{\theta} = \arg\max_{\theta\in\Theta} \pi(\theta|y) = \arg\max_{\theta\in\Theta} \pi(y|\theta).\pi_0(\theta)$$

$$= \arg\min_{\theta\in\Theta} \left[\underbrace{\left(\mathcal{M}(\theta,e)\right)-y)^T \left[\Sigma_m+\Sigma_y\right]^{-1}\left(\mathcal{M}(\theta,e)\right)-y)}_{\text{Least-square term (Mahalanobis distance)}} + \underbrace{\left(\theta-\bar{\theta}\right)^T \Sigma_0^{-1}\left(\theta-\bar{\theta}\right)}_{\text{Regularization term}} \right] \tag{22}$$

This way, the structure of the constitutive relation is imposed strongly, and it is assumed to know the modeling error features, which is not the case in most problems. To avoid this issue, the mCRE strategy integrates modeling error in a global manner that allows for more flexibility in the model structure. To the modeling error (the CRE) is thus associated a pdf to globally quantify the confidence on the less reliable parts of the model:

$$\pi_{CRE} \propto \exp\left[\frac{-1}{\alpha}\zeta^2(s,\theta)\right] \tag{23}$$

The confidence on the modeling exponentially decreases when the CRE value increases, with a rate speed specified by the scalar α. Therefore, in a mCRE context with a measurement error norm based on the covariance of the measurements Σ_y, one can rewrite the likelihood pdf:

$$\pi(y|\theta) \propto \exp\left[-\frac{1}{2}\left(\mathcal{M}(\theta,e)\right)-y\right)^T\Sigma_y^{-1}\left(\mathcal{M}(\theta,e)\right)-y)\right].\exp\left[\frac{-1}{\alpha}\zeta^2(s,\theta)\right] \tag{24}$$

for any admissible mechanical solution s. Thus, if one no longer assumes any a priori on θ (uniform pdf), the application of the MAP principle leads to:

$$\hat{\theta} = \underset{\theta\in\Theta}{\arg\min}\left[\left(\mathcal{M}(\theta,e)\right)-y\right)^T\Sigma_y^{-1}\left(\mathcal{M}(\theta,e)\right)-y) + \frac{1}{\alpha}\zeta^2(s,\theta)\right] \tag{25}$$

where one easily recognizes the sum of a model error (the CRE) with a data-to-model distance to minimize. It thus illustrates that the mCRE metric can be closely related to the Bayesian inference framework.

4.2. mCRE-based OSP: modified Fisher Information Matrix

The key idea of the proposed sensor placement technique is to use the mechanical fields $\{U_\omega\}_{\omega\in D_\omega}$ computed for mCRE needs within the Information Entropy concept. Mathematically, we thus define a modified Fisher Information Matrix Q_m such that:

$$Q_m = \sum_{\omega\in D_\omega}\left(\Pi\nabla_\theta U_\omega\right)^T\left(\Pi\Sigma_y\Pi^T\right)^{-1}\left(\Pi\nabla_\theta U_\omega\right) \tag{26}$$

In other words, the modified FIM analyzes the sensitivity of the mCRE measurement error part with respect to the parameters to identify. The effect of the CRE is implicit in the computation of U_ω. Similarly to former OSP techniques, the determinant of the modified FIM is maximized to optimally position sensors (assuming the amount of data is large enough to reuse the asymptotic result mentioned above). In the following, we will consider the positioning of a limited number of sensors on a predefined grid on possible locations. In that context, it has been shown in the literature [28] that FSSP provides almost-optimal results compared to GA in reasonable CPU times. This justifies the use of this optimization strategy in the following, although all the previously mentioned sensor placement algorithmic structures are applicable (only the FIM definition is changed). Alg. 2 presents the iterative mCRE-based FSSP process. It is worth noticing that the access to a semi-analytical expression of the gradient of U_ω with respect to θ is a valuable asset to perform OSP in reasonable CPU times: the modified FIM Q_m can thus be computed quickly without any loss of precision. One should notice that the computation of $\nabla_\theta U_\omega$ is a low-cost post-processing operation once (18) has been solved (see Appendix A for mathematical developments).

5. Application to accelerometer optimal placement for damage detection

5.1. Description of the problem

A typical earthquake engineering application is considered here with the frame structure of Fig. 1 submitted to a tridimensional low-magnitude random ground acceleration. Such input

Algorithm 2: mCRE-based FSSP algorithm

Initialization:

- Grid of all N_d possible sensors locations
- Targeted number of sensors N_s
- Number of selected sensors $n = 0$
- Initial parameter guess $\theta_0 \in \Theta$
- Set of simulated measurements y (obtained with θ_0)
- FE model including mesh and matrices K, D, M
- mCRE tuning parameters: frequency bandwidth D_ω, confidence into measurements scalar α, frequency weighting function $z(\omega)$

while $n < N_s$ **do**

  Consider all possible combinations by adding one new sensor: $\{\Pi_j\}_{j\in[\![1;N_d-n]\!]}$

  for $j \in [\![1; N_d - n]\!]$ **do**

    Initialize the modified FIM $Q_{m,j} = 0$

    for $\omega \in D_\omega$ **do**

      Get mechanical fields (U_ω, V_ω) solving the $AX = b$ system (equation 18)

      Compute $\nabla_\theta U_\omega$ (equation 41)

      $Q_{m,j} = Q_{m,j} + (\Pi_j \nabla_\theta U_\omega)^T (\Pi_j \Sigma_y \Pi_j^T)^{-1} (\Pi_j \nabla_\theta U_\omega)$

    end

  end

  Identify the sensor configuration $J = \underset{j\in[\![1;N_d-n]\!]}{\arg\min} \{\det(Q_{m,j})\}$

  Store the new sensor of configuration J as the $(n+1)^{th}$ optimal position

  Go to the next iteration: $n \to n+1$

end

signals are used in Earthquake Engineering experiments to perform modal identification [76] once damage has occured. The objective of this study is to position at best a restricted budget of accelerometers in order to identify accurately the uncertain stiffness distribution of the structure in forthcoming (possibly damaging) experiments. As we assume that very few sensors are available, an intuitive coarse stiffness parametrization of the stiffness is proposed: 6 subdomains are defined {W10, W11, W20, W21, F10, F20}, one per wall and per slab. The updated stiffness model (12) is thus made of $N_\theta = 6$ parameters. The subdomains areas are shown in FIG. 1. The model is made of shell elements using the CEA modeling software CAST3M© [77]. Relative time acceleration measurements in both x and y directions are simulated using Fast Fourier Transforms and the direct dynamics problem formulated in terms of relative displacement is:

$$M\ddot{x} + D\dot{x} + K(\theta)x(t) = -M\Xi\ddot{u}_d \ , \quad x = u - u_d \tag{27}$$

where Ξ is a matrix addressing the acceleration ground motion to the associated dofs and $\ddot{u}_d$ the random ground acceleration input constructed as a multivariate zero-mean Gaussian process.

The objective of this application is to assess the proposed sensor placement strategy for efficient mCRE-based identification. To restrain CPU times and avoid sensors concentrations, we define a grid on 48 potential sensor locations: a triaxial accelerometer can be positioned at each orange dof of FIG. 1.

Although several types of sensors could be positioned simultaneously, only accelerometers are considered herein because they are a popular, minimally invasive and easily deployable sensing devices for SHM and Earthquake Engineering applications. In order to be realistic regarding what could be achieved in practical shaking table tests, a restricted budget of $N_s = 24$ data acquisition channels has been fixed. $N_s = 24$ allows to uniformly spread enough sensors to reproduce typical sensor placement configurations that are done in earthquake engineering applications. Besides, as $N_\theta = 6$ parameters are supposed to be updated, it is theoretically enough to get proper identification results and redundancy in the information carried out by

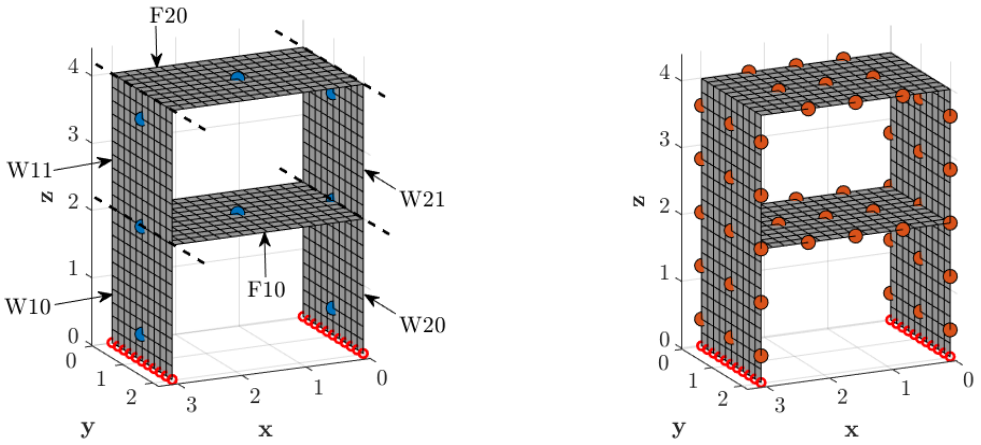

(a) Frame with uniform sensor placement (blue dots).

(b) Grid of possible accelerometer locations.

FIGURE 1: Frame structure - uniform default sensor placement and grid of possible locations for OSP. Subdomains areas and denomination are also given.

measurements.

5.2. OSP benchmark

In order to assess the relevance of mCRE-based OSP with respect to other OSP strategies, a numerical benchmark has been conducted to perform and compare sensor placements oriented towards different quantities of interest. An overview of the tested strategies is presented in TAB. 2. A FSSP optimization algorithm is used in all cases to fairly compare sensor placement results between methods. As a reminder, it has been shown many times in the literature that FSSP has similar performance with GA, particularly when the number of sensors to position remains small [**?**].

Description and desingation		**Optimality criterion**	**Accelerometer type**
Reference richest OSP ($N_s = 48$)	Ref	-	-
Uniform default OSP	Def	-	Triaxial
OSP for modal analysis of the 10 first structural eigenmodes	MA1	$\log(\det Q(\Phi))$	Uniaxial
	MA2		Triaxial
OSP for standard structural identification	SI1	$\log(\det Q(X))$	Uniaxial
	SI2		Triaxial
mCRE-based OSP	mCRE1	$\log(\det Q_m)$	Uniaxial
	mCRE2		Triaxial
mCRE-based OSP for uncertain damage scenarios	mCRE-MS1	$\int_\Theta \log(\det Q_m)\pi_0(\theta)\mathrm{d}\theta$	Uniaxial
	mCRE-MS2		Triaxial

TABLE 2: OSP benchmark

Among the proposed sensor placement strategies, it should be highlighted that:

- ▷ In the reference richest OSP, all the possible locations are covered with triaxial accelerometers, meaning $N_s = 48$ in that case. This is not a realistic configuration, neither an economous one, but it allows to provide results that will be used as reference when comparing the performance of OSPs in terms of model updating.
- ▷ In the uniform default case, 8 triaxial accelerometers are uniformly spread over the structure. This is typically what should be done naively without considering OSP algorithms in practice.

▷ Optimal uniaxial and triaxial accelerometer placement are systematically compared. Of course, positioning triaxial sensors is much more convenient from the experimental viewpoint, as it is less constraining for the instrumentalists. Besides, it is less computationally demanding than uniaxial accelerometer placement because the number of possible sensor configurations is reduced. However, forcing triaxial sensors implies the addition of constraints to OSP strategies, which should thus lead to less performant results as less freedom is given to the sensor plan.

▷ The OSP strategies oriented towards modal analysis aim at identifying at best the 10 first structural eigenmodes. The latter are stored in the modeshape matrix Φ, and the associated Fisher Information Matrix reads:

$$Q(\Phi) = (\Pi\Phi)^T \left(\Pi\Sigma_y\Pi^T\right)^{-1} (\Pi\Phi) \tag{28}$$

which is independent of the nominal stiffness parameter values θ_0. In addition, the optimal sensor locations are also independent of the excitation used. The FIM in that case has exactly the same form as the one proposed for the EI method [19]. Finally, as 10 modes are stored in Φ, one should expect to get singular FIM while less than 10 sensors have not been positioned on the specimen. To avoid numerical issues, the determinant of the FIM will be computed as the product of the non-zero eigenvalues of $Q(\Phi)$.

▷ The OSP for structural identification directly deals with the identification (in a least-square sense) of the stiffness parameters. In that case, the FIM is directly computed from the sensitivity of the frequency-domain counterpart of the mechanical state X with respect to the parameter set θ:

$$Q(X) = \sum_{\omega\in D_\omega} (\Pi\nabla_\theta X_\omega)^T \left(\Pi\Sigma_y\Pi^T\right)^{-1} (\Pi\nabla_\theta X_\omega) \tag{29}$$

with (for the considered stiffness parametrization):

$$\nabla_\theta X_\omega = -\left[-\omega^2 M + i\omega D + K(\theta)\right]^{-1} \frac{\partial K}{\partial \theta} \left[-\omega^2 M + i\omega D + K(\theta)\right]^{-1} \left[\omega^2 M \Xi U_{d,\omega}\right] \tag{30}$$

For legitimate comparisons with mCRE-based OSP, the frequency range that is considered to compute $Q(X)$ is also D_ω. Note that the FIM could also be obtained with time-domain measurements, but the sensitivity matrix would be obtained solving a (more expensive) full time domain problem [39].

Contrary to the MA cases, the optimal sensor locations depend on the location and type of excitation that is used. Also, the matrix $Q(X)$ may be non-singular even for only one positioned sensor since the structural response obtained from the model may store enough information from all contributing eigenmodes in order to estimate the parameter set θ.

▷ Regarding the settings of the mCRE, as the first five modes of the structure are below 20 Hz and are the most sollicitated ones, a frequency bandwidth $D_\omega = [1\text{ Hz}; 30\text{ Hz}]$ with $\Delta f = 0.1$ Hz has been chosen for the computation of all forthcoming results. The call to a reduced basis made of the first 20 eigenmodes of the frame allows to achieve fast and accurate mCRE computations as it largely covers the frequency range of interest. The weighting function $z(\omega)$ is computed using the complex modal indicator function as explained in [78]. α will be subject to calibration tests, therefore its value will be specified afterwards.

▷ Because one also intends to provide sensor placements that are still efficient once damage has occurred, the case of multiple scenarios mCRE-based optimal sensor placement has been addressed. Following the subdomain decomposition shown in Fig. 1, the 6 parameters have been pseudo-randomly sampled using a Latin Hypercube algorithm in order to

take into consideration 30 damage scenarios, assuming the parameter set follows a multivariate uniform pdf on [0.2;1]. A uniform prior pdf has been chosen due to the fact it is the less informative in the sense of the statistical maximum entropy. The generated set of samples is denoted Θ_s. Each $\theta_s \in \Theta_s$ is thus used to simulate a dataset y_s, which will be processed to perform OSP. The stiffness parametrization of each scenario is given in Fig. 2. The change on stiffness parameters has significant effects on the frequency domain response of the structure as one can observe in Fig. 3 where the normalized H-CMIF plot for each considered damage configuration is given [46]. The latter is defined as the dominant singular value of the transfer function from the crossed input/output PSD matrices. It is called H-CMIF because of its similarities with the Complex Modal Identification Function [79]. The frequency shift of the H-CMIF peaks shows how the structural response varies from one scenario to the other.

Following the work initiated in [27] for the case of highly uncertain parameters, the optimality criterion is thus approximated by:

$$\int_{\Theta} \log\left(\det\left(Q_m(\Pi,\theta,y)\right)\right)\pi(\theta)\mathrm{d}\theta \approx \frac{1}{\mathrm{card}(\Theta_s)} \sum_{\theta_s\in\Theta_s} \log\left(\det(Q_m(\Pi,\theta_s,y_s(\theta_s)))\right) \tag{31}$$

leading to an optimal sensor placement that is dedicated to a wider range of damage configurations. In practice, it is true that cases involving damage at the top of the structure are highly unlikely, but the uncertainty on parameters provided by this approach enables to take modeling bias into consideration. As a last remark, although not considered here because of the assumed non-damaging nature of the input signals, the variability of loading conditions may also have been exploited if nonlinear damaging models were used, so that the damage scenarios that are generated for OSP are much more realistic.

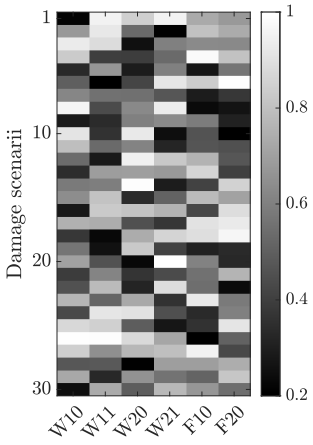

Figure 2: Stiffness samples Θ_s to simulate multiple damage scenarios.

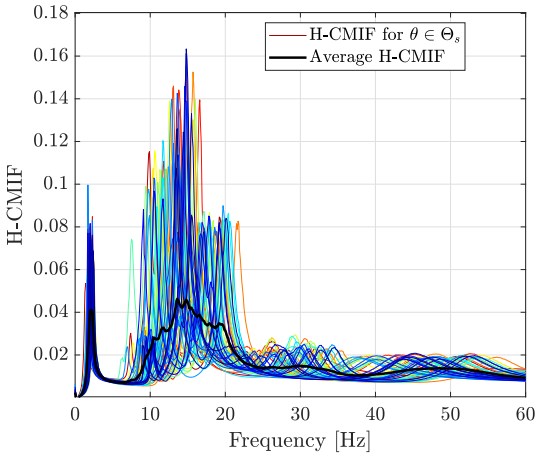

Figure 3: Impact of damage configuration on the frequency response of the structure. A wide variability of responses is integrated into the OSP framework.

5.3. OSP results - first comments

5.3.1. Modal identification

The OSP results obtained for modal analysis using a truncated modal basis made of the first 10 modes of the frame are presented in Fig. 4. To confirm the soundness of the results, we plot both $\det(Q)$ and the CMIF obtained after having positioned accelerometers with comparison to the one obained with the rich OSP configuration.

The amount of information carried by the first sensors is more important as it allows the identification of one supplementary mode. When as many sensors as modes in Φ have been

positioned, the additional information carried by new sensors is less important as it only conforts the modal identification, making it more accurate. Due to the complexity of the structure, no clear visual trend from the sensor position can be easily guessed, except that most sensors are located on the floors. This appears to be quite natural as floor eigenmodes are part of the 10 first ones of the structure.

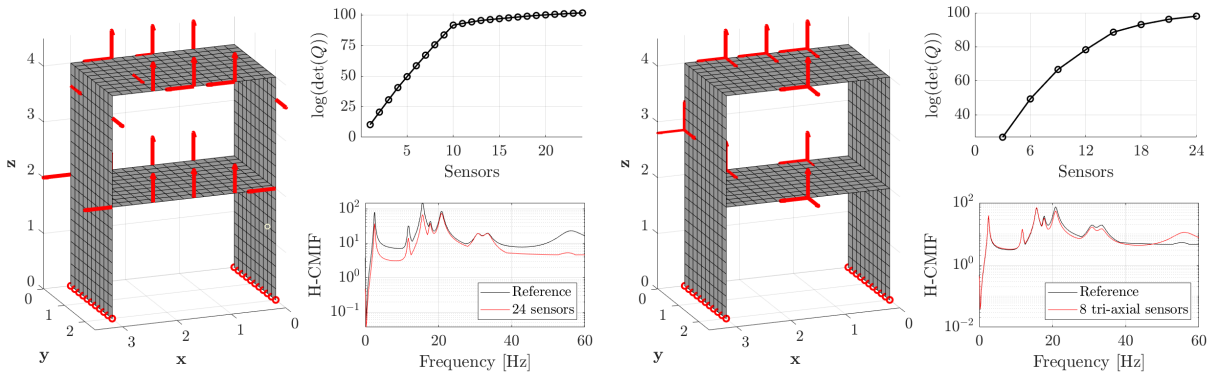

FIGURE 4: OSP of uniaxial and triaxial accelerometers for the MA1 (left) and MA2 cases (right). Accelerometers positions and orientations are given by the red arrows, while determinant of the FIM (in log scale) and H-CMIF are plotted to confirm the soundness of the approach.

5.4. Structural identification OSP results

The OSP results obtained for SI1 and SI2 cases are presented in FIG. 5. The evolution of $\det(Q(X))$ is also given to confirm the relevance of the results. Due to the large parameters sensitivity, the sensor placement is not visually intuitive in the sense that not all subdomains are covered by at least one sensor. One can interpret the fact that sensors are mostly located at the top of the structure because it remains the most kinematically responsive part of the latter. However, from the sudden slope change of the determinant of the FIM with positioned sensors, we find that after the placement of 6 sensors, the system is a priori totally identifiable, meaning that new sensors bring (mostly) redundant information. As a remark, note that the values of $\det(Q(X))$ between the modal analysis OSP and structural identification OSP are not comparable as the FIM definition is different.

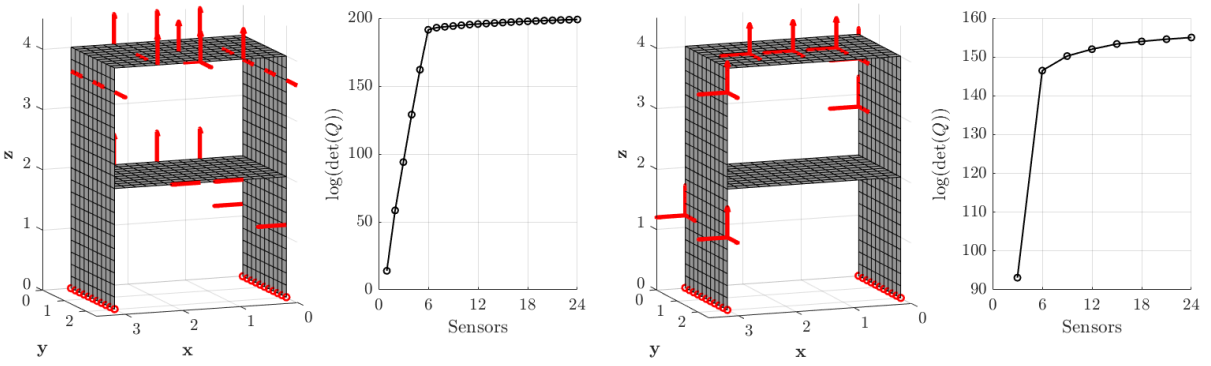

FIGURE 5: OSP of uniaxial and triaxial accelerometers for the SI1 (left) and SI2 cases (right). Accelerometers positions and orientations are given by the red arrows, and the determinant of the FIM (in log scale) is plotted to confirm the soundness of the approach.

5.4.1. mCRE-based OSP results

The OSP results obtained for mCRE1 and mCRE2 cases are presented in Fig. 6. To understand at best the sensor placement process, a particular attention was paid to the sequential positioning of sensors by coloring the sensor position according to their order of appearance in the FSSP algorithm. The value of the det (Q_m) is also provided. The mCRE settings that allowed to provide the following results are given above. The value of α is well-known to be crucial in the mCRE framework, and as it is not properly tunable at the experimental design stage, its influence on mCRE-based OSP results was explicitely studied. What can be observed at first glance is that the more important the confidence into measurements α, the closer to the bottom of the structure for sensor locations. If the increasing value of $\det(Q_m)$ confirms FSSP behaves correctly, the values plotted in Fig. 6 are not comparable as they are function of α. For the following studies, the confidence into measurements coefficient has been chosen at $\alpha = 10^4$ because of the correct dispersion of the sensors on the whole structure (see Fig. 6).

Finally, OSP results for mCRE-based sensor placement taking multiple damage scenarios into account are presented in Fig. 7. Several remarks can be made from theses placements. First, there is no sensor positioned in the x direction for the mCRE-MS1 case, which can explain why the mCRE-MS2 sensor placement is much less optimal in the sense of the criterion to maximize. Unsurprisingly, it is interesting to notice that the first sensors in both cases are located at the bottom of the structure, where damage is most likely to occur. Similarly, few sensors are located on the top walls as they are less identifiable (in the CRE sense) and less prone to damage. Of course, the numerical resources that are necessary to compute these results are much more important, as it requires $\mathrm{card}(\Theta_s)$ times more solutions of the mCRE system. Hopefully the required CPU time did not exceed more than 12 hours on a personal laptop. This numerical effort should be worthwhile, as the resulting sensor placement will be effective over a wider range of stiffness configurations.

5.5. Assessment of sensor configurations for mCRE-based model updating

5.5.1. Model updating contexts

Because we look for optimal sensor placement in the sense of damage detection, we propose to challenge the different OSP that have been obtained and presented previously for mCRE-based model updating using three datasets that fairly represent the typical situations one can meet in practice:

(i) Updating the model from the same data that has been used to perform OSP. The expected parameter vector is exactly the one that has been used to position sensors.

(ii) Updating the model from data obtained after an overall 10% stiffness underestimation. This is a situation that can be encountered if model bias is present. Measurements include in that case additional noise for which ratio of standard deviation with input standard deviation is 10%.

(iii) Updating the model from data obtained in a new damaged scenario. The expected parameter vector is $\theta^\star = [0.5\ 0.9\ 0.6\ 0.9\ 0.8\ 1]$. Measurements are also polluted with noise (10% in level too).

Case (i) is probably the most comfortable model updating situation with high-quality measurements; Case (ii) gets more difficult as noise is added to measurements and a uniform model bias must be recovered; Case (iii) is the most challenging problem as a damaged configuration must be identified from noisy measurements using sensors whose positions have been optimized from a totally different parameter estimate (except for mCRE-MS1 and mCRE-MS2 cases). Because of the random nature of measurement noise, one cannot expect to properly assess model updating performance exclusively with parameters estimates. Model updating results will thus

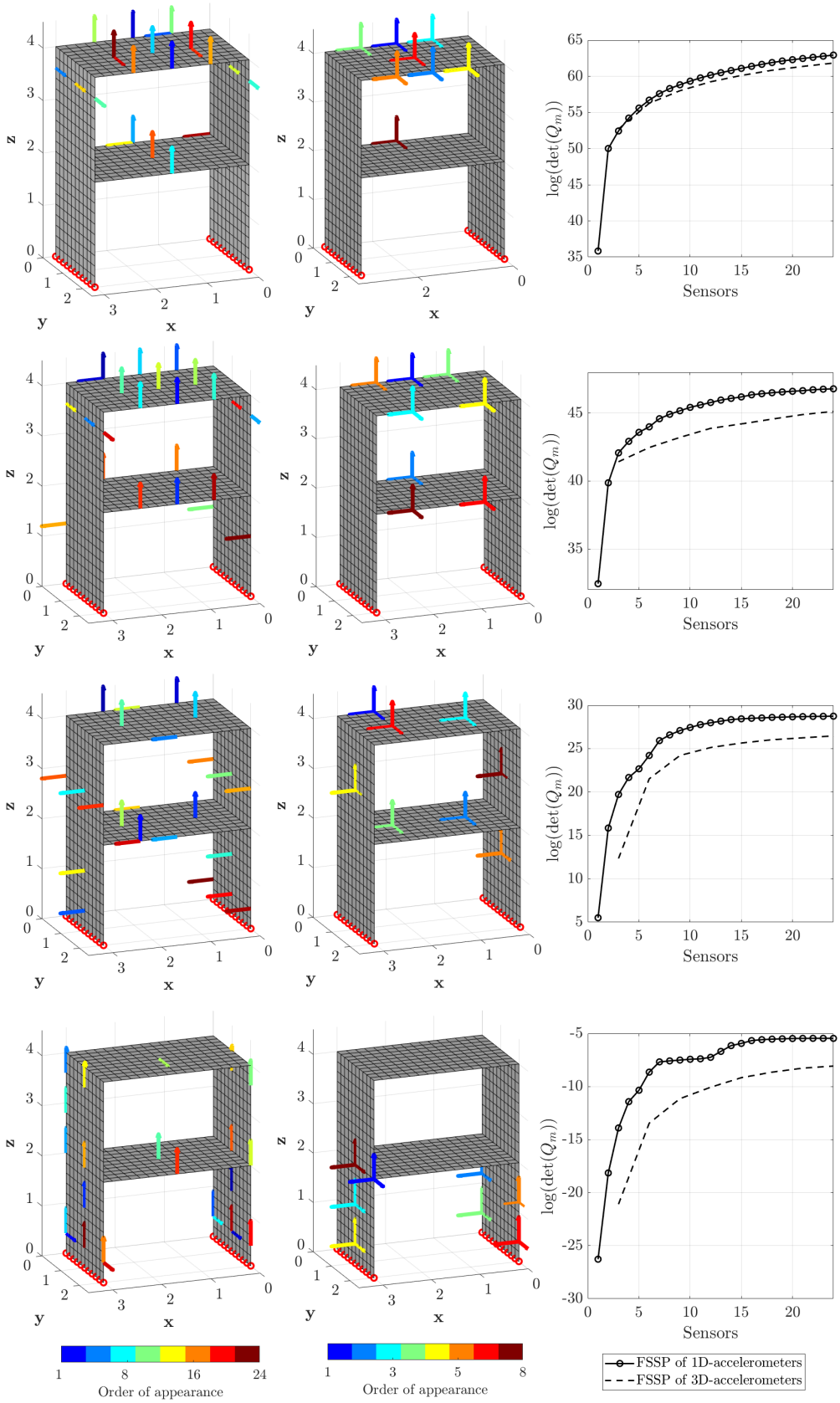

FIGURE 6: mCRE-based OSP of uniaxial and triaxial accelerometers for the identification of the 6-subdomain parametrization of the frame. The arrows indicate the sensor position and their color indicates their order of appearance in the FSSP strategy. From top to bottom, results have been obtained with $\alpha = \{1; 10^2; 10^4; 10^6\}$.

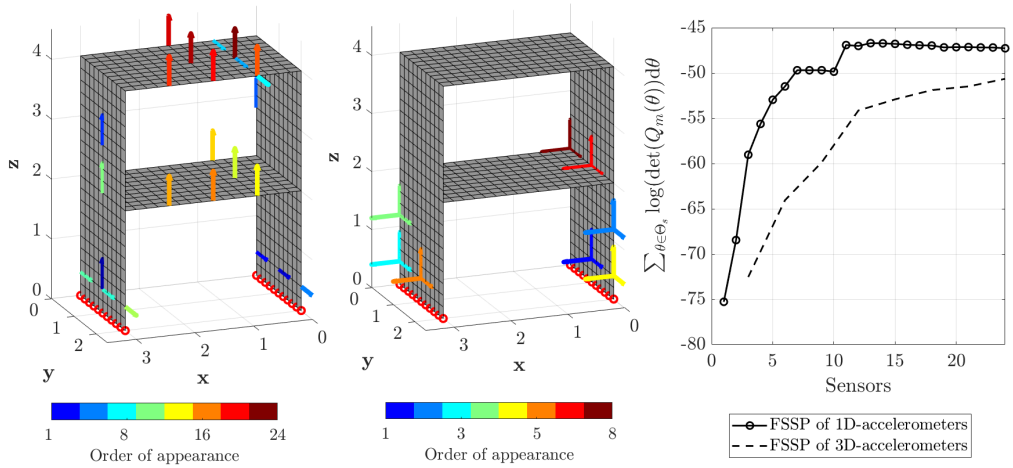

FIGURE 7: mCRE-based OSP of uniaxial and triaxial accelerometers taking multiple damage scenarios into account. The arrows indicate the sensor position and their color indicates their order of appearance in the FSSP strategy. A value of $\alpha = 10^4$ was chosen.

be assessed using both parameter estimates and relative confidence intervals widths, using the richest sensor placement as reference.

The assessment of OSP for model updating is summarized in FIG. 8 with 6 colormaps. For each model updating scenario, we propose two colormaps: the first one indicates the relative gap in [%] of parameter estimates with respect to the exact parameter set that should have been recovered $\theta^\star$ (see FIG. 8.a). The second one shows the relative width in [%] of confidence intervals with respect to the ones given by the reference sensor placement configuration (see FIG. 8.b and Appendix B for mathematical details).

For all maps, each line indicates the performance obtained by a given sensor placement (denominations are given in TAB. 2) while each column corresponds to a given subdomain (denominations are given in FIG. 1).

The understanding of results displayed in FIG. 8.b is not direct and is recalled in the following lines: a close-to-zero value means that the convexity of the mCRE functional evaluated around $\hat{\theta}$ with a given OSP is almost the same as the one of the mCRE evaluated with the reference sensor placement case in which twice the number of sensors are present. It suggests that the considered sensor placement is efficient in the sense that there is not much additional doubt regarding the value of parameter estimate. On the contrary, when the relative gap on confidence intervals width is important, the mCRE functional is less convex around $\hat{\theta}$, meaning that another measurement noise realization may have lead to significantly different model updating results.

5.5.2. Discussion on the relevance of the modified FIM

Several conclusions can be drawn from the results shown in FIG. 8. First, because the number of sensors ($N_s = 24$) was sufficiently important with respect to the number of parameters to be identified ($N_\theta = 6$), correct mCRE-based model updating results have been obtained in all cases as parameters have been correctly identified with less than 10% error with respect to the expected values in the most unfavorable case. The comparison of the maps (a.i) and (a.ii) reveals that the presence of noise extends the identification issues on the less sensitive parameters of the problem, namely the top-story ones (W11, W21 and F20). Besides, if one compares the visual positioning of sensors previously shown with the relative confidence intervals widths, it appears that the subdomains of parameters having large intervals are not directly equipped by sensors (associated to poor local convexity of the functional and low sensitivity). One can also observe that the sensor placement configurations constrained to triaxial accelerometers are less efficient, as expected from the values of the determinant of the FIM plotted in the FSSP results.

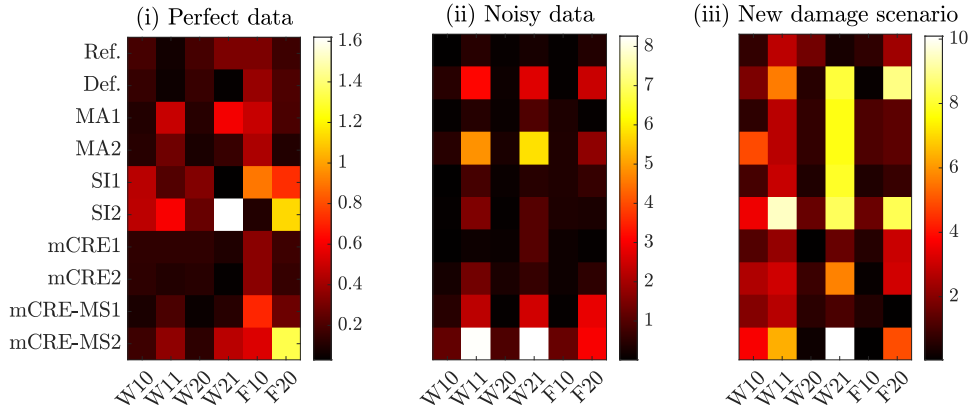

(a) Relative gaps on parameter estimates (in [%]) obtained with the different sensor configurations.

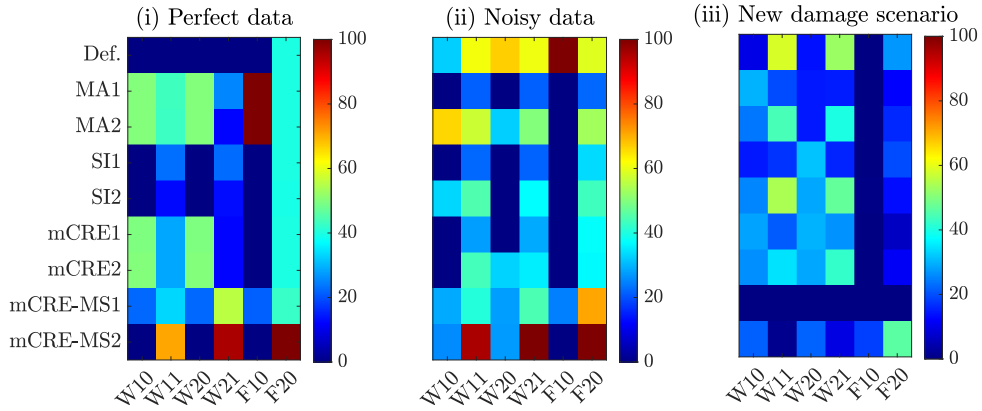

(b) Relative gaps on confidence intervals (in [%]) obtained with the different sensor configurations.

FIGURE 8: Assessment of sensor placements for several mCRE-based model updating problems.

The overall analysis of FIG. 8 confirms the effectiveness of mCRE-based OSP. Indeed, mCRE1 and mCRE2 sensor configurations provide the best parameter estimates, with minimal confidence intervals when data is noisy. This application is thus a proof of concept showing the benefits of FSSP with the modified FIM that directly yields from the interpretation of mCRE from a Bayesian viewpoint. Nevertheless, it is important to keep in mind the main limitation of this new OSP approach: the strong dependency in the confidence into measurements coefficient α. As running a mCRE-based OSP algorithm did not last more than 5 minutes for the considered case, the experimental designer can afford to assess mCRE-based OSPs obtained for several values of α. Despite this alternative, in-depth studies must be conducted to clarify this point. In particular, one can legitimately wonder if the optimality criteria for calibrating α that has been recently proposed in [80] are convenient to obtain relevant sensor configurations.

Finally, let us point out that taking into account several damage scenarios allows for a more robust sensor placement with respect to the identification of new parameter configurations, as shown in the FIG. 8 - mCRE-MS1 case at scenario (iii), where the identification is almost perfect with minimal confidence intervals. The computational time spent to "learn" the best trade-off from multiple datasets is thus worth of interest. As one could have expected, taking into account several scenarios makes mCRE-MS1 and mCRE-MS2 model updating results sub-optimal (yet efficient) for cases (i) and (ii) compared to mCRE1 and mCRE2. However, the performance achieved in case (iii) by mCRE-MS1 and mCRE-MS2 is remarkable and promising for monitoring the occurrence and evolution of structural defects on structures. This observation goes in the sense of recent contributions [71, 66] which emphasize the need to take both model and measurement uncertainties into consideration to build efficient and robust OSP.

6. Conclusion and prospects

The ambition of this paper consisted in the development of a novel sensor placement algorithm that is dedicated to mCRE-based model updating. Owing to the link between the mCRE (though deterministic) and the Bayesian inference framework, and inspired from the Information Entropy concept, a modified Fisher Information Matrix was introduced and its determinant was maximized to optimally position sensors in the mCRE sense. A proof of concept showing the relevance of this new mCRE-based OSP strategy has been proposed on a 3D academic example where we sought for optimal accelerometers locations on a two-story frame structure subjected to random ground motion. This case study permitted to perform deep analysis of this new OSP approach and to compare it with other classical techniques in different model updating scenarios. In particular, the effect of the confidence into measurements coefficient has been emphasized, as well as the fact to take into consideration multiple scenarios so as to anticipate a wider range of potential damage occurences. OSP methods were compared in terms of mCRE-based model updating from different datasets, which allowed to illustrate the efficiency and relevance of the proposed mCRE-based OSP methodology. If this study focuses on accelerometers as they are common and weakly invasive for earthquake engineering applications, all types of sensors can be easily integrated in the proposed framework.

Consequently, the proposed mCRE-based OSP appears as an interesting additional asset for the construction of a mCRE-unified framework for SHM or structural dynamics applications (see Fig. 9 for an example on how OSP could be combined to the recent publications of the authors [46, 72]). However, there is no doubt that this tool still lacks of maturity to be properly exploited, and further research should address the strong influence of the confidence into measurements coefficient [80]. Besides, as OSP are not exclusively intended to perform optimal model updating, future work will focus on finding the best sensor placement trade-off that contributes to multiple objectives simultaneously, for example modal identification and mCRE-based model updating. Pareto front algorithms may be a first tool for this purpose. Finally, one of the current on-going investigations of the authors concerns the use of mCRE-based OSP for active sensing purposes in order to improve damage detection in cases where the state of the structure is tracked online via data assimilation techniques [72]. Iterative strategies could then be employed to refine the sensor configuration only where needed, *i.e.* where damage occurences are detected.

Appendix A Analytical expressions of the mCRE derivatives

Before providing gradient and Hessian matrix analytical expressions, let us recall that we are dealing with quantities written in the frequency domain. Therefore, derivatives must be considered with caution: the real and imaginary parts have to be separated to write consistent mathematical expressions (in particular Gateaux's derivatives). In the following, $\bullet_r$ and $\bullet_i$ will denote the real and imaginary parts of $\bullet$, respectively. Besides, indices ω will be omitted for the sake of clarity as all forthcoming developments are one at a given angular frequency ω. In particular, one can rewrite the system (18) so as to exhibit explicitly real and imaginary parts of U and V in a decoupled manner:

$$
\begin{aligned}
&A_{\text{ext}}(\theta)X_{\text{ext}} = b_{\text{ext}} \text{ with} \\
&A_{\text{ext}}(\theta) = \begin{bmatrix} K(\theta)-\omega^2 M+\alpha\Pi^T G\Pi & -(K(\theta)-\omega^2 M) & \omega D & -\omega D \\ -\omega^2 M & K(\theta) & -\omega D & 0 \\ -\omega D & \omega D & K(\theta)-\omega^2 M+\alpha\Pi^T G\Pi & -(K(\theta)-\omega^2 M) \\ \omega D & 0 & -\omega^2 M & K(\theta) \end{bmatrix} \\
&X_{\text{ext}}^T = \begin{bmatrix} U_r^T & V_r^T & U_i^T & V_i^T \end{bmatrix} \\
&b_{\text{ext}}^T = \begin{bmatrix} \alpha Y^T G\Pi & F_r^T & 0 & F_i^T \end{bmatrix}
\end{aligned}
\tag{32}
$$

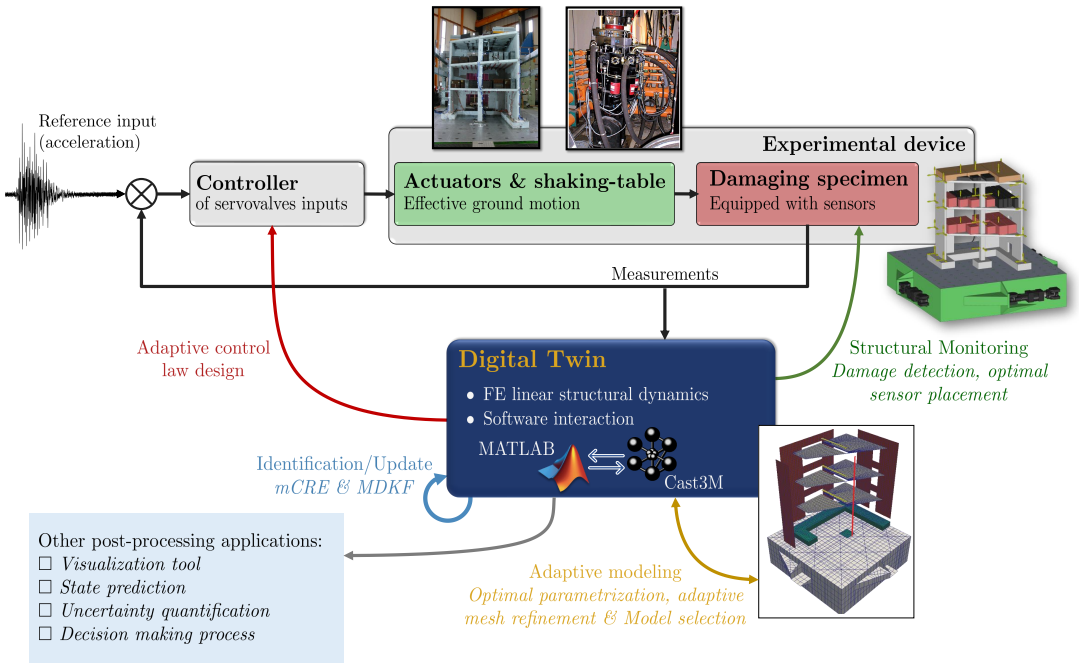

FIGURE 9: Long-term perspective: enhanced shaking-table experiments with a unified framework based on the modified Constitutive Relation Error.

A.1 Analytical mCRE gradient

Once the mechanicals fields $\widehat{s} = (U, V)$ are computed, the expression of the mCRE gradient with respect to the parameters to update can be analytical (only if the link between stiffness and parameters is too).

$$\left.\frac{\mathrm{d}e_\omega^2}{\mathrm{d}\theta}\right|_{\widehat{s}} \triangleq \left.\frac{\mathrm{d}\mathcal{L}}{\mathrm{d}\theta}\right|_{\widehat{s}} = \frac{\partial e_\omega^2}{\partial \theta} + \underbrace{\frac{\partial \mathcal{L}}{\partial U_r}\frac{\mathrm{d}U_r}{\mathrm{d}\theta} + \frac{\partial \mathcal{L}}{\partial V_r}\frac{\mathrm{d}V_r}{\mathrm{d}\theta} + \frac{\partial \mathcal{L}}{\partial U_i}\frac{\mathrm{d}U_i}{\mathrm{d}\theta} + \frac{\partial \mathcal{L}}{\partial V_i}\frac{\mathrm{d}V_i}{\mathrm{d}\theta}}_{=0 \text{ at the saddle point}} \tag{33}$$

As the parameters weight the FE stiffness matrix, a general formulation for the mCRE gradient with respect to parameter $\theta_k, k \in [\![1; n_\theta]\!]$ is:

$$\left.\frac{\mathrm{d}e_\omega^2}{\mathrm{d}\theta_k}\right|_{\widehat{s}} = \frac{1}{2}\left[U_r^T\frac{\partial K}{\partial \theta_k}U_r + U_i^T\frac{\partial K}{\partial \theta_k}U_i - V_r^T\frac{\partial K}{\partial \theta_k}V_r - V_i^T\frac{\partial K}{\partial \theta_k}V_i\right] \tag{34}$$

For the stiffness parametrization (12), one thus directly gets:

$$\left.\frac{\mathrm{d}e_\omega^2}{\mathrm{d}\theta_k}\right|_{\widehat{s}} = \frac{1}{2}\left[U_r^T K_{0,k}U_r + U_i^T K_{0,k}U_i - V_r^T K_{0,k}V_r - V_i^T K_{0,k}V_i\right] \tag{35}$$

The possibility to provide an analytical gradient when minimizing the mCRE is thus strongly recommended due to its simplicity of implementation as well as the associated computational speed-up.

A.2 Semi-analytical Hessian matrix

Following the same idea, the mCRE Hessian matrix value at coordinate $j,k \in [\![1;n_\theta]\!]^2$ reads:

$$\begin{aligned}\mathcal{H}^\theta_{jk} = \left.\frac{\mathrm{d}^2 e^2_\omega}{\mathrm{d}\theta_j \mathrm{d}\theta_k}\right|_{\widehat{s}} \triangleq \frac{\mathrm{d}^2\mathcal{L}}{\mathrm{d}\theta_j\mathrm{d}\theta_k} = \frac{\partial^2\mathcal{L}}{\partial\theta_j\partial\theta_k} &+ \left[\frac{\mathrm{d}}{\mathrm{d}U_r}\left(\frac{\partial\mathcal{L}}{\partial\theta_k}\right)\right]^T\frac{\mathrm{d}U_r}{\mathrm{d}\theta_j} + \left[\frac{\mathrm{d}}{\mathrm{d}V_r}\left(\frac{\partial\mathcal{L}}{\partial\theta_k}\right)\right]^T\frac{\mathrm{d}V_r}{\mathrm{d}\theta_j}\\ &+ \left[\frac{\mathrm{d}}{\mathrm{d}U_i}\left(\frac{\partial\mathcal{L}}{\partial\theta_k}\right)\right]^T\frac{\mathrm{d}U_i}{\mathrm{d}\theta_j} + \left[\frac{\mathrm{d}}{\mathrm{d}V_i}\left(\frac{\partial\mathcal{L}}{\partial\theta_k}\right)\right]^T\frac{\mathrm{d}V_i}{\mathrm{d}\theta_j}\end{aligned} \tag{36}$$

Three terms to develop thus occur:

- The second order partial derivative of the augmented cost-function $\mathcal{L}$, which is trivial:

$$\frac{\partial^2\mathcal{L}}{\partial\theta_j\partial\theta_k} = \frac{1}{2}\left[U_r^T\frac{\partial^2 K}{\partial\theta_j\partial\theta_k}U_r + U_i^T\frac{\partial^2 K}{\partial\theta_j\partial\theta_k}U_i - V_r^T\frac{\partial^2 K}{\partial\theta_j\partial\theta_k}V_r - V_i^T\frac{\partial^2 K}{\partial\theta_j\partial\theta_k}V_i\right] \tag{37}$$

- The crossed derivatives, whose computation is also direct:

$$\begin{cases}\dfrac{\mathrm{d}}{\mathrm{d}U_r}\left(\dfrac{\partial\mathcal{L}}{\partial\theta_k}\right) &= \dfrac{\partial K}{\partial\theta_k}U_r\\ \dfrac{\mathrm{d}}{\mathrm{d}V_r}\left(\dfrac{\partial\mathcal{L}}{\partial\theta_k}\right) &= -\dfrac{\partial K}{\partial\theta_k}V_r\\ \dfrac{\mathrm{d}}{\mathrm{d}U_i}\left(\dfrac{\partial\mathcal{L}}{\partial\theta_k}\right) &= \dfrac{\partial K}{\partial\theta_k}U_i\\ \dfrac{\mathrm{d}}{\mathrm{d}V_i}\left(\dfrac{\partial\mathcal{L}}{\partial\theta_k}\right) &= -\dfrac{\partial K}{\partial\theta_k}V_i\end{cases} \tag{38}$$

- The derivatives of $\widehat{s}$ with respect to parameters, whose computation can be obtained by derivation of the system $A_{\text{ext}}X_{\text{ext}} = b_{\text{ext}}$:

$$\frac{\mathrm{d}A_{\text{ext}}}{\mathrm{d}\theta_j}X_{\text{ext}} + A_{\text{ext}}\frac{\mathrm{d}X_{\text{ext}}}{\mathrm{d}\theta_j} = \frac{\mathrm{d}b_{\text{ext}}}{\mathrm{d}\theta_j} \Rightarrow \frac{\mathrm{d}X_{\text{ext}}}{\mathrm{d}\theta_j} = A^{-1}_{\text{ext}}\left[\frac{\mathrm{d}b_{\text{ext}}}{\mathrm{d}\theta_j} - \frac{\mathrm{d}A_{\text{ext}}}{\mathrm{d}\theta_j}X_{\text{ext}}\right] \tag{39}$$

with A^{-1}_{ext} that can be already known from the $A_{\text{ext}}X_{\text{ext}} = b_{\text{ext}}$ solution to compute the mCRE value (*i.e.* the inverse matrix can be stored) and:

$$\begin{cases}\dfrac{\mathrm{d}b_{\text{ext}}}{\mathrm{d}\theta_j} &= 0\\ \dfrac{\mathrm{d}A_{\text{ext}}}{\mathrm{d}\theta_j} &= \begin{bmatrix}\frac{\partial K}{\partial\theta_j} & -\frac{\partial K}{\partial\theta_j} & 0 & 0\\ 0 & \frac{\partial K}{\partial\theta_j} & 0 & 0\\ 0 & 0 & \frac{\partial K}{\partial\theta_j} & -\frac{\partial K}{\partial\theta_j}\\ 0 & 0 & 0 & \frac{\partial K}{\partial\theta_j}\end{bmatrix}\end{cases} \tag{40}$$

All simplifications done, one obtains:

$$\frac{\mathrm{d}}{\mathrm{d}\theta_j}\begin{bmatrix}U_r\\ V_r\\ U_i\\ V_i\end{bmatrix} = -A^{-1}_{\text{ext}}\begin{bmatrix}\dfrac{\partial K}{\partial\theta_j}(U_r - V_r)\\ \dfrac{\partial K}{\partial\theta_j}V_r\\ \dfrac{\partial K}{\partial\theta_j}(U_i - V_i)\\ \dfrac{\partial K}{\partial\theta_j}V_i\end{bmatrix} \tag{41}$$

Finally, the general expression of $\mathcal{H}^{\theta}_{jk}$ reads:

$$\mathcal{H}^{\theta}_{jk} = \frac{1}{2}\left[U_r^T \frac{\partial^2 K}{\partial\theta_j\partial\theta_k} U_r + U_i^T \frac{\partial^2 K}{\partial\theta_j\partial\theta_k} U_i - V_r^T \frac{\partial^2 K}{\partial\theta_j\partial\theta_k} V_r - V_i^T \frac{\partial^2 K}{\partial\theta_j\partial\theta_k} V_i\right] - \begin{bmatrix} \frac{\partial K}{\partial\theta_k} U_r \\ -\frac{\partial K}{\partial\theta_k} V_r \\ \frac{\partial K}{\partial\theta_k} U_i \\ -\frac{\partial K}{\partial\theta_k} V_i \end{bmatrix}^T A^{-1}_{\text{ext}} \begin{bmatrix} \frac{\partial K}{\partial\theta_j}(U_r - V_r) \\ \frac{\partial K}{\partial\theta_j} V_r \\ \frac{\partial K}{\partial\theta_j}(U_i - V_i) \\ \frac{\partial K}{\partial\theta_j} V_i \end{bmatrix} \tag{42}$$

The application of this expression to the stiffness parametrization (12) leads to:

$$\mathcal{H}^{\theta}_{jk} = -\begin{bmatrix} K_{0,k} U_r \\ -K_{0,k} V_r \\ K_{0,k} U_i \\ -K_{0,k} V_i \end{bmatrix}^T A^{-1}_{\text{ext}} \begin{bmatrix} K_{0,j}(U_r - V_r) \\ K_{0,j} V_r \\ K_{0,j}(U_i - V_i) \\ K_{0,j} V_i \end{bmatrix} \tag{43}$$

If the expression of the mCRE gradient is easily available (according to the stiffness parametrization), the mCRE gradient with respect to updated parameters must be provided to minimization algorithms in order to get enhanced numerical performances. The case of the Hessian matrix is a bit different due to the fact that it requires intelligent storage of the inverse matrix of A_{ext} for all $\omega \in D_\omega$. In particular, one can notice that A is inverted instead of A_{ext} due to its reduced size. Of course, providing the Hessian would also reduce the amount of iterations of nonlinear optimization algorithms but it also carries a storage burden that should be taken into account as A^{-1}_{ext} must be stored and differs for all $\omega \in D_\omega$.

Appendix B Confidence intervals to assess mCRE-based model updating in terms of relative uncertainty

As explained in [52], providing optimal parameters inside confidence intervals is an original and effective way to deal with the uncertainty associated with the FE model as well as excitation levels with a low computational cost, as it is a one-step direct post-processing procedure to perform once the model updating algorithm has minimized the mCRE funcitonal $\mathcal{J}$. At the converged point $\widehat{\theta}$, using the convexity properties of the functional, there exists a subset $I_\theta \subset \Theta$ of finite size such that:

$$\forall\ \theta \in I_\theta, \quad \mathcal{J}(\theta) < \epsilon.\mathcal{J}(\widehat{\theta}) \tag{44}$$

where ϵ is a constant scalar. The width of I_θ for a given threshold ϵ can be established using a second order Taylor polynomial approximation around the optimal parameters $\widehat{\theta}$:

$$\mathcal{J}(\theta) = J(\theta) + \mathcal{O}\left((\theta - \widehat{\theta})^3\right) \text{ with } J(\theta) = \mathcal{J}(\widehat{\theta}) + \left[\frac{\mathrm{d}\mathcal{J}}{\mathrm{d}\theta}\right]^T (\theta - \widehat{\theta}) + \frac{1}{2}(\theta - \widehat{\theta})^T \left[\frac{\mathrm{d}^2\mathcal{J}}{\mathrm{d}^2\theta}\right](\theta - \widehat{\theta}) \tag{45}$$

Once gradient and Hessian matrix are supplied, the 2nd order approximation of the mCRE is directly available, which allows to calculate the size of I_θ for all parameters (ϵ has to be user-defined).

Note that the proposed confidence intervals are not rigorously able to quantify uncertainties on $\widehat{\theta}$. Nonetheless, they are enough to draw preliminary conclusions about the relative ability to identify parameters: comparing the relative width of confidence intervals allows to assess which parameters are subjected to more doubt than others. This can be helpful if one wants to focus model updating actions on exclusively highly-sensitive parameters in order to avoid physically-meaningless local minima.

References

[1] J. Brownjohn, Structural health monitoring of civil infrastructure, Philosophical Transactions of the Royal Society A: Mathematical, Physical and Engineering Sciences 365 (1851) (2007) 589–622. doi:10.1098/rsta.2006.1925.
URL https://royalsocietypublishing.org/doi/10.1098/rsta.2006.1925

[2] S. Laflamme, L. Cao, E. Chatzi, F. Ubertini, Damage Detection and Localization from Dense Network of Strain Sensors, Shock and Vibration 2016 (2016) 1–13. doi:10.1155/2016/2562949.
URL http://www.hindawi.com/journals/sv/2016/2562949/

[3] G. F. Gomes, Y. A. D. Mendez, P. da Silva Lopes Alexandrino, S. S. da Cunha, A. C. Ancelotti, A Review of Vibration Based Inverse Methods for Damage Detection and Identification in Mechanical Structures Using Optimization Algorithms and ANN, Archives of Computational Methods in Engineering 26 (4) (2019) 883–897. doi:10.1007/s11831-018-9273-4.
URL https://doi.org/10.1007/s11831-018-9273-4

[4] E. N. Chatzi, M. N. Chatzis, C. Papadimitriou (Eds.), Robust Monitoring, Diagnostic Methods and Tools for Engineered Systems, Frontiers Research Topics, Frontiers Media SA, 2020. doi:10.3389/978-2-88966-088-9.

[5] E. Simoen, G. De Roeck, G. Lombaert, Dealing with uncertainty in model updating for damage assessment: A review, Mechanical Systems and Signal Processing 56-57 (2015) 123–149. doi:10.1016/j.ymssp.2014.11.001.
URL https://linkinghub.elsevier.com/retrieve/pii/S0888327014004130

[6] W. Fan, P. Qiao, Vibration-based Damage Identification Methods: A Review and Comparative Study, Structural Health Monitoring 10 (1) (2011) 83–111, publisher: SAGE Publications. doi:10.1177/1475921710365419.
URL https://doi.org/10.1177/1475921710365419

[7] J. E. Mottershead, M. I. Friswell, Model Updating In Structural Dynamics: A Survey, Journal of Sound and Vibration 167 (2) (1993) 347–375. doi:10.1006/jsvi.1993.1340.
URL https://www.sciencedirect.com/science/article/pii/S0022460X83713404

[8] A. Tarantola, Inverse Problem Theory and Methods for Model Parameter Estimation, Society for Industrial and Applied Mathematics, 2005. doi:10.1137/1.9780898717921.
URL http://epubs.siam.org/doi/book/10.1137/1.9780898717921

[9] M. I. Friswell, Damage identification using inverse methods, Philosophical Transactions of the Royal Society A: Mathematical, Physical and Engineering Sciences 365 (1851) (2007) 393–410. doi:10.1098/rsta.2006.1930.
URL https://royalsocietypublishing.org/doi/10.1098/rsta.2006.1930

[10] A. Bensoussan, Optimization of sensor's location in a distributed filtering problem., Stability of stochastic dynamical systems (1972) 62–84.

[11] T. K. Yu, J. H. Seinfled, Observability and optimal measurement location in linear distributed parameter systems, International Journal of Control 18 (4) (1973) 785–799, publisher: Taylor & Francis _eprint: https://doi.org/10.1080/00207177308932556. doi:10.1080/00207177308932556.
URL https://doi.org/10.1080/00207177308932556

[12] T.-H. Yi, H.-N. Li, Methodology Developments in Sensor Placement for Health Monitoring of Civil Infrastructures, International Journal of Distributed Sensor Networks 8 (8) (2012) 612726, publisher: SAGE Publications. doi:10.1155/2012/612726.
URL https://doi.org/10.1155/2012/612726

[13] V. Mallardo, M. Aliabadi, Optimal Sensor Placement for Structural, Damage and Impact Identification: A Review, Structural Durability & Health Monitoring 9 (4) (2013) 287–323. doi:10.32604/sdhm.2013.009.287.
URL http://www.techscience.com/sdhm/v9n4/35096

[14] W. Ostachowicz, R. Soman, P. Malinowski, Optimization of sensor placement for structural health monitoring: a review, Structural Health Monitoring 18 (3) (2019) 963–988, publisher: SAGE Publications. doi:10.1177/1475921719825601.
URL https://doi.org/10.1177/1475921719825601

[15] R. J. Barthorpe, K. Worden, Emerging Trends in Optimal Structural Health Monitoring System Design: From Sensor Placement to System Evaluation, Journal of Sensor and Actuator Networks 9 (3) (2020) 31, number: 3 Publisher: Multidisciplinary Digital Publishing Institute. doi:10.3390/jsan9030031.
URL https://www.mdpi.com/2224-2708/9/3/31

[16] P. Cawley, R. D. Adams, The location of defects in structures from measurements of natural frequencies, The Journal of Strain Analysis for Engineering Design 14 (2) (1979) 49–57, publisher: IMECHE. doi:10.1243/03093247V142049.
URL https://doi.org/10.1243/03093247V142049

[17] P. C. Shah, F. E. Udwadia, A Methodology for Optimal Sensor Locations for Identification of Dynamic Systems, Journal of Applied Mechanics 45 (1) (1978) 188–196. doi:10.1115/1.3424225.
URL https://doi.org/10.1115/1.3424225

[18] P. Kirkegaard, R. Brincker, On the optimal location of sensors for parametric identification of linear structural systems, Mechanical Systems and Signal Processing 8 (6) (1994) 639–647. doi:10.1006/mssp.1994.1045.
URL https://linkinghub.elsevier.com/retrieve/pii/S0888327084710454

[19] D. C. Kammer, Sensor placement for on-orbit modal identification and correlation of large space structures, Journal of Guidance, Control, and Dynamics 14 (2) (1991) 251–259. doi:10.2514/3.20635.
URL https://arc.aiaa.org/doi/abs/10.2514/3.20635

[20] E. Heredia-Zavoni, L. Esteva, Optimal instrumentation of uncertain structural systems subject to earthquake ground motions, Earthquake Engineering & Structural Dynamics 27 (4) (1998) 343–362. doi:10.1002/(SICI)1096-9845(199804)27:4<343::AID-EQE726>3.0.CO;2-F.
URL https://onlinelibrary.wiley.com/doi/abs/10.1002/%28SICI%291096-9845%28199804%2927%3A4%3C343%3A%3AAID-EQE726%3E3.0.CO%3B2-F

[21] F. E. Udwadia, Methodology for Optimum Sensor Locations for Parameter Identification in Dynamic Systems, Journal of Engineering Mechanics 120 (2) (1994) 368–390, publisher: American Society of Civil Engineers. doi:10.1061/(ASCE)0733-9399(1994)120:2(368).
URL https://ascelibrary.org/doi/abs/10.1061/%28ASCE%290733-9399%281994%29120%3A2%28368%29

[22] E. Heredia-Zavoni, R. Montes-Iturrizaga, L. Esteva, Optimal instrumentation of structures on flexible base for system identification, Earthquake Engineering & Structural Dynamics 28 (12) (1999) 1471–1482. doi:10.1002/(SICI)1096-9845(199912)28:12<1471::AID-EQE872>3.0.CO;2-M.
URL https://onlinelibrary.wiley.com/doi/abs/10.1002/%28SICI%291096-9845%28199912%2928%3A12%3C1471%3A%3AAID-EQE872%3E3.0.CO%3B2-M

[23] M. Reynier, H. Abou-kandil, Sensors Location For Updating Problems, Mechanical Systems and Signal Processing 13 (2) (1999) 297–314. doi:10.1006/mssp.1998.1213.
URL https://www.sciencedirect.com/science/article/pii/S0888327098912134

[24] L. Yao, W. A. Sethares, D. C. Kammer, Sensor placement for on-orbit modal identification via a genetic algorithm, AIAA Journal 31 (10) (1993) 1922–1928, publisher: American Institute of Aeronautics and Astronautics _eprint: https://doi.org/10.2514/3.11868. doi:10.2514/3.11868.
URL https://doi.org/10.2514/3.11868

[25] J. L. Beck, L. S. Katafygiotis, Updating Models and Their Uncertainties. I: Bayesian Statistical Framework, Journal of Engineering Mechanics 124 (4) (1998) 455–461, publisher: American Society of Civil Engineers. doi:10.1061/(ASCE)0733-9399(1998)124:4(455).
URL https://ascelibrary.org/doi/abs/10.1061/%28ASCE%290733-9399%281998%29124%3A4%28455%29

[26] L. S. Katafygiotis, J. L. Beck, Updating Models and Their Uncertainties. II: Model Identifiability, Journal of Engineering Mechanics 124 (4) (1998) 463–467, publisher: American Society of Civil Engineers. doi:10.1061/(ASCE)0733-9399(1998)124:4(463).
URL https://ascelibrary.org/doi/abs/10.1061/%28ASCE%290733-9399%281998%29124%3A4%28463%29

[27] C. Papadimitriou, J. L. Beck, S.-K. Au, Entropy-Based Optimal Sensor Location for Structural Model Updating, Journal of Vibration and Control 6 (5) (2000) 781–800, publisher: SAGE Publications Ltd STM. doi:10.1177/107754630000600508.
URL https://doi.org/10.1177/107754630000600508

[28] C. Papadimitriou, Optimal sensor placement methodology for parametric identification of structural systems, Journal of Sound and Vibration 278 (4) (2004) 923–947. doi:10.1016/j.jsv.2003.10.063.
URL https://www.sciencedirect.com/science/article/pii/S0022460X04000355

[29] H. Y. Guo, L. Zhang, L. L. Zhang, J. X. Zhou, Optimal placement of sensors for structural health monitoring using improved genetic algorithms, Smart Materials and Structures 13 (3) (2004) 528–534, publisher: IOP Publishing. doi:10.1088/0964-1726/13/3/011.
URL https://doi.org/10.1088/0964-1726/13/3/011

[30] K. Zhou, Z. Wu, X. Yi, D. Zhu, R. Narayan, J. Zhao, Generic Framework of Sensor Placement Optimization for Structural Health Modeling, Journal of Computing in Civil Engineering 31 (2017) 04017018. doi:10.1061/(ASCE)CP.1943-5487.0000662.

[31] A. Mendler, M. DÃ¶hler, C. E. Ventura, Sensor placement with optimal damage detectability for statistical damage detection, Mechanical Systems and Signal Processing 170 (2022) 108767. doi:10.1016/j.ymssp.2021.108767.
URL https://www.sciencedirect.com/science/article/pii/S0888327021010815

[32] M. Azarbayejani, A. I. El-Osery, K. K. Choi, M. M. R. Taha, A probabilistic approach for optimal sensor allocation in structural health monitoring, Smart Materials and Structures 17 (5) (2008) 055019, publisher: IOP Publishing. doi:10.1088/0964-1726/17/5/055019.
URL https://doi.org/10.1088/0964-1726/17/5/055019

[33] K. Worden, A. P. Burrows, Optimal sensor placement for fault detection, Engineering Structures 23 (8) (2001) 885–901. doi:10.1016/S0141-0296(00)00118-8.
URL https://www.sciencedirect.com/science/article/pii/S0141029600001188

[34] M. Bruggi, S. Mariani, Optimization of sensor placement to detect damage in flexible plates, Engineering Optimization 45 (6) (2013) 659–676, publisher: Taylor & Francis _eprint: https://doi.org/10.1080/0305215X.2012.690870. doi:10.1080/0305215X.2012.690870.
URL https://doi.org/10.1080/0305215X.2012.690870

[35] B. Blachowski, M. Ostrowski, P. Tauzowski, A. Swiercz, L. Jankowski, Sensor placement for structural damage identification by means of topology optimization, AIP Conference Proceedings 2239 (1) (2020) 020002, publisher: American Institute of Physics. doi:10.1063/5.0007817.
URL https://aip.scitation.org/doi/abs/10.1063/5.0007817

[36] D. Nasr, R. E. Dahr, J. Assaad, J. Khatib, Comparative Analysis between Genetic Algorithm and Simulated Annealing-Based Frameworks for Optimal Sensor Placement and Structural Health Monitoring Purposes, Buildings 12 (9) (2022) 1383. doi:10.3390/buildings12091383.
URL https://www.mdpi.com/2075-5309/12/9/1383

[37] J. M. Beal, A. Shukla, O. A. Brezhneva, M. A. Abramson, Optimal sensor placement for enhancing sensitivity toÂ change in stiffness for structural health monitoring, Optimization and Engineering 9 (2) (2008) 119–142. doi:10.1007/s11081-007-9023-1.
URL https://doi.org/10.1007/s11081-007-9023-1

[38] C. Papadimitriou, Pareto optimal sensor locations for structural identification, Computer Methods in Applied Mechanics and Engineering 194 (12) (2005) 1655–1673. doi:10.1016/j.cma.2004.06.043.
URL https://www.sciencedirect.com/science/article/pii/S0045782504004104

[39] C. Papadimitriou, G. Lombaert, The effect of prediction error correlation on optimal sensor placement in structural dynamics, Mechanical Systems and Signal Processing 28 (2012) 105–127. doi:10.1016/j.ymssp.2011.05.019.
URL https://linkinghub.elsevier.com/retrieve/pii/S0888327011002214

[40] J. E. Mottershead, M. Link, M. I. Friswell, The sensitivity method in finite element model updating: A tutorial, Mechanical Systems and Signal Processing 25 (7) (2011) 2275–2296. doi:10.1016/j.ymssp.2010.10.012.
URL https://linkinghub.elsevier.com/retrieve/pii/S0888327010003316

[41] B. Titurus, M. I. Friswell, Regularization in model updating, International Journal for Numerical Methods in Engineering 75 (4) (2008) 440–478. doi:10.1002/nme.2257.
URL https://onlinelibrary.wiley.com/doi/10.1002/nme.2257

[42] B. Weber, P. Paultre, J. Proulx, Consistent regularization of nonlinear model updating for damage identification, Mechanical Systems and Signal Processing 23 (6) (2009) 1965–1985. doi:10.1016/j.ymssp.2008.04.011.
URL https://www.sciencedirect.com/science/article/pii/S088832700800109X

[43] C. D. Zhang, Y. L. Xu, Comparative studies on damage identification with Tikhonov regularization and sparse regularization: Damage Detection with Tikhonov Regularization and Sparse Regularization, Structural Control and Health Monitoring 23 (3) (2016) 560–579. doi:10.1002/stc.1785.
URL https://onlinelibrary.wiley.com/doi/10.1002/stc.1785

[44] S. Huang, P. Feissel, P. Villon, Modified constitutive relation error: An identification framework dealing with the reliability of information, Computer Methods in Applied Mechanics and Engineering 311 (2016) 1–17. doi:10.1016/j.cma.2016.06.030.
URL https://linkinghub.elsevier.com/retrieve/pii/S0045782516306557

[45] T. Silva, N. Maia, Detection and localisation of structural damage based on the error in the constitutive relations in dynamics, Applied Mathematical Modelling 46 (2017) 736–749. doi:10.1016/j.apm.2016.07.002.
URL https://linkinghub.elsevier.com/retrieve/pii/S0307904X16303833

[46] M. Diaz, P.-E. Charbonnel, L. Chamoin, Robust energy-based model updating framework for random processes in dynamics: application to shaking-table experiments, Computers and Structures 264 (106746) (2022) 40. doi:https://doi.org/10.1016/j.compstruc.2022.106746.

[47] A. T. Chouaki, P. Ladevèze, L. Proslier, Updating Structural Dynamic Models with Emphasis on the Damping Properties, AIAA Journal 36 (6) (1998) 1094–1099, publisher: American Institute of Aeronautics and Astronautics _eprint: https://doi.org/10.2514/2.486. doi:10.2514/2.486.
URL https://doi.org/10.2514/2.486

[48] P. Ladevèze, A. Chouaki, Application of a posteriori error estimation for structural model updating, Inverse Problems 15 (1) (1999) 49–58, publisher: IOP Publishing. doi:10.1088/0266-5611/15/1/009.
URL https://doi.org/10.1088/0266-5611/15/1/009

[49] P. Ladevèze, D. Leguillon, Error Estimate Procedure in the Finite Element Method and Applications, SIAM Journal on Numerical Analysis 20 (3) (1983) 485–509, publisher: Society for Industrial and Applied Mathematics. doi:10.1137/0720033.
URL https://epubs.siam.org/doi/10.1137/0720033

[50] W. Aquino, M. Bonnet, Analysis of the error in constitutive equation approach for time-harmonic elasticity imaging, SIAM Journal on Applied Mathematics 79 (3) (2019) 822–849. arXiv:https://doi.org/10.1137/18M1231237, doi:10.1137/18M1231237.
URL https://doi.org/10.1137/18M1231237

[51] P. Feissel, O. Allix, Modified constitutive relation error identification strategy for transient dynamics with corrupted data: The elastic case, Computer Methods in Applied Mechanics and Engineering 196 (13-16) (2007) 1968–1983. doi:10.1016/j.cma.2006.10.005.
URL https://linkinghub.elsevier.com/retrieve/pii/S0045782506003434

[52] P. Charbonnel, P. Ladevèze, F. Louf, C. Le Noac'h, A robust CRE-based approach for model updating using in situ measurements, Computers & Structures 129 (2013) 63–73. doi:10.1016/j.compstruc.2013.08.002.
URL https://linkinghub.elsevier.com/retrieve/pii/S0045794913002216

[53] E. Barbarella, O. Allix, F. Daghia, J. Lamon, T. Jollivet, A new inverse approach for the localization and characterization of defects based on compressive experiments, Computational Mechanics 57 (6) (2016) 1061–1074. doi:10.1007/s00466-016-1278-y.
URL http://link.springer.com/10.1007/s00466-016-1278-y

[54] X. Hu, S. Prabhu, S. Atamturktur, S. Cogan, Mechanistically-informed damage detection using dynamic measurements: Extended constitutive relation error, Mechanical Systems and Signal Processing 85 (2017) 312–328. doi:10.1016/j.ymssp.2016.08.013.
URL https://linkinghub.elsevier.com/retrieve/pii/S0888327016302965

[55] B. Banerjee, T. F. Walsh, W. Aquino, M. Bonnet, Large scale parameter estimation problems in frequency-domain elastodynamics using an error in constitutive equation functional, Computer Methods in Applied Mechanics and Engineering 253 (2013) 60–72. doi:10.1016/j.cma.2012.08.023.
URL https://linkinghub.elsevier.com/retrieve/pii/S0045782512002770

[56] R. Ferrier, A. Cocchi, C. Hochard, Modified constitutive relation error for field identification: Theoretical and experimental assessments on fiber orientation identification in a composite material, International Journal for Numerical Methods in Engineering (2021). doi:10.1002/nme.6842.
URL https://onlinelibrary.wiley.com/doi/10.1002/nme.6842

[57] J. Waeytens, B. Rosić, P.-E. Charbonnel, E. Merliot, D. Siegert, X. Chapeleau, R. Vidal, V. le Corvec, L.-M. Cottineau, Model updating techniques for damage detection in concrete beam using optical fiber strain measurement device, Engineering Structures 129 (2016) 2–10. doi:10.1016/j.engstruct.2016.08.004.
URL https://linkinghub.elsevier.com/retrieve/pii/S0141029616304059

[58] Z. Y. Shi, S. S. Law, L. M. Zhang, Optimum Sensor Placement for Structural Damage Detection, Journal of Engineering Mechanics 126 (11) (2000) 1173–1179, publisher: American Society of Civil Engineers. doi:10.1061/(ASCE)0733-9399(2000)126:11(1173).
URL https://ascelibrary.org/doi/abs/10.1061/%28ASCE%290733-9399%282000%29126%3A11%281173%29

[59] B. Blachowski, Modal Sensitivity Based Sensor Placement for Damage Identification Under Sparsity Constraint, Periodica Polytechnica Civil Engineering (Mar. 2019). doi:10.3311/PPci.13888.
URL https://pp.bme.hu/ci/article/view/13888

[60] D. C. Kammer, Effect of model error on sensor placement for on-orbit modal identification of large space structures, Journal of Guidance, Control, and Dynamics 15 (2) (1992) 334–341, publisher: American Institute of Aeronautics and Astronautics _eprint: https://doi.org/10.2514/3.20841. doi:10.2514/3.20841.
URL https://doi.org/10.2514/3.20841

[61] D. C. Kammer, Effects of Noise on Sensor Placement for On-Orbit Modal Identification of Large Space Structures, Journal of Dynamic Systems, Measurement, and Control 114 (3) (1992) 436–443. doi:10.1115/1.2897366.
URL https://doi.org/10.1115/1.2897366

[62] D. C. Kammer, M. L. Tinker, Optimal placement of triaxial accelerometers for modal vibration tests, Mechanical Systems and Signal Processing 18 (1) (2004) 29–41. doi:10.1016/S0888-3270(03)00017-7.
URL https://www.sciencedirect.com/science/article/pii/S0888327003000177

[63] M. Salama, T. Rose, J. Garba, Optimal placement of excitations and sensors for verification of large dynamical systems, in: 28th Structures, Structural Dynamics and Materials Conference, American Institute of Aeronautics and Astronautics, 1987. doi:https://doi.org/10.2514/6.1987-782.
URL https://arc.aiaa.org/doi/abs/10.2514/6.1987-782

[64] D. S. Li, H. N. Li, C. P. Fritzen, The connection between effective independence and modal kinetic energy methods for sensor placement, Journal of Sound and Vibration 305 (4) (2007) 945–955. doi:10.1016/j.jsv.2007.05.004.
URL https://www.sciencedirect.com/science/article/pii/S0022460X07003537

[65] K.-V. Yuen, L. S. Katafygiotis, C. Papadimitriou, N. C. Mickleborough, Optimal Sensor Placement Methodology for Identification with Unmeasured Excitation, Journal of Dynamic Systems, Measurement, and Control 123 (4) (2001) 677–686. doi:10.1115/1.1410929.
URL https://doi.org/10.1115/1.1410929

[66] S. Cantero-Chinchilla, J. L. Beck, M. Chiachío, J. Chiachío, D. Chronopoulos, A. Jones, Optimal sensor and actuator placement for structural health monitoring via an efficient convex cost-benefit optimization, Mechanical Systems and Signal Processing 144, publisher: Elsevier (Apr. 2020). doi:10.1016/j.ymssp.2020.106901.

[67] P. Metallidis, G. Verros, S. Natsiavas, C. Papadimitriou, Fault Detection and Optimal Sensor Location in Vehicle Suspensions, Journal of Vibration and Control 9 (3-4) (2003) 337–359, publisher: SAGE Publications Ltd STM. doi:10.1177/107754603030755.
URL https://doi.org/10.1177/107754603030755

[68] Q. Long, M. Motamed, R. Tempone, Fast Bayesian optimal experimental design for seismic source inversion, Computer Methods in Applied Mechanics and Engineering 291 (2015) 123–145. doi:10.1016/j.cma.2015.03.021.
URL https://www.sciencedirect.com/science/article/pii/S0045782515001310

[69] T. Yin, K.-V. Yuen, H.-F. Lam, H.-p. Zhu, Entropy-Based Optimal Sensor Placement for Model Identification of Periodic Structures Endowed with Bolted Joints, Computer-Aided Civil and Infrastructure Engineering 32 (12) (2017) 1007–1024. doi:10.1111/mice.12309.
URL https://onlinelibrary.wiley.com/doi/10.1111/mice.12309

[70] C. Argyris, S. Chowdhury, V. Zabel, C. Papadimitriou, Bayesian optimal sensor placement for crack identification in structures using strain measurements, Structural Control and Health Monitoring 25 (5) (2018) e2137. doi:10.1002/stc.2137.
URL https://onlinelibrary.wiley.com/doi/abs/10.1002/stc.2137

[71] T. Ercan, C. Papadimitriou, Optimal Sensor Placement for Reliable Virtual Sensing Using Modal Expansion and Information Theory, Sensors 21 (10) (2021) 3400, number: 10 Publisher: Multidisciplinary Digital Publishing Institute. doi:10.3390/s21103400.
URL https://www.mdpi.com/1424-8220/21/10/3400

[72] M. Diaz, P.-E. Charbonnel, L. Chamoin, A new kalman filter approach for structural parameter tracking: Application to the monitoring of damaging structures tested on shaking-tables, Mechanical Systems and Signal Processing 182 (2023) 109529. doi:https://doi.org/10.1016/j.ymssp.2022.109529.
URL https://www.sciencedirect.com/science/article/pii/S088832702200632X

[73] A. Deraemaeker, P. Ladevèze, P. Leconte, Reduced bases for model updating in structural dynamics based on constitutive relation error, Computer Methods in Applied Mechanics and Engineering 191 (21-22) (2002) 2427–2444. doi:10.1016/S0045-7825(01)00421-2.
URL https://linkinghub.elsevier.com/retrieve/pii/S0045782501004212

[74] A. Deraemaeker, P. Ladevèze, T. Romeuf, Model validation in the presence of uncertain experimental data, Engineering Computations 21 (8) (2004) 808–833. doi:10.1108/02644400410554335.
URL https://www.emerald.com/insight/content/doi/10.1108/02644400410554335/full/html

[75] H. N. Nguyen, L. Chamoin, C. Ha Minh, mcre-based parameter identification from full-field measurements: Consistent framework, integrated version, and extension to nonlinear material behaviors, Computer Methods in Applied Mechanics and Engineering 400 (2022) 115461. doi:https://doi.org/10.1016/j.cma.2022.115461.
URL https://www.sciencedirect.com/science/article/pii/S0045782522004947

[76] P.-E. Charbonnel, Fuzzy-driven strategy for fully automated modal analysis: Application to the SMART2013 shaking-table test campaign, Mechanical Systems and Signal Processing 152 (2021) 107388. doi:10.1016/j.ymssp.2020.107388.
URL https://linkinghub.elsevier.com/retrieve/pii/S0888327020307743

[77] Cast3M, http://www-cast3m.cea.fr.

[78] C. Y. Shih, Y. G. Tsuei, R. J. Allemang, D. L. Brown, Complex mode indication function and its applications to spatial domain parameter estimation, Mechanical Systems and Signal Processing 2 (4) (1988) 367–377. doi:10.1016/0888-3270(88)90060-X.
URL https://www.sciencedirect.com/science/article/pii/088832708890060X

[79] R. J. Allemang, D. L. Brown, A Complete Review of the Complex Mode Indicator Function (CMIF) with Applications (2006) 38.
URL https://www.semanticscholar.org/paper/A-Complete-Review-of-the-Complex-Mode-Indicator-(-)-Allemang-Brown/5184ead6fcde301507bad9aa09b6bce08d97dceb

[80] M. Diaz, P.-É. Charbonnel, L. Chamoin, Fully automated physics-regularized model updating algorithm for vibration-based damage detection from sparse dataSubmitted - preprint avalaible on HAL (03872031) (2022).